University of Crete

Undergraduate Thesis

PT plasmons in rectangular and twist geometries

Author: Sygrimis Andrianos-Ilias

Supervisor: Prof. Tsironis Giorgos

Committee Member: Prof. Makris Konstantinos

Committee Member: Prof. Tzortzakis Stelios

Acknowledgementes

I would like to deeply thank my supervisor and mentor Prof. Giorgos Tsironis for his support and guidance during my thesis. I would also like to thank Dr. Marios Mattheakis for his collaboration and knowledge obtained through our discussions. I would also like to thank my colleagues Michalis Dramitinos and Panagiotis Karavelas for their support during my thesis and the large number of discussions and trades of knowledge to each other during that period. Last, I would like to thank Amalia for her support.

Contents

1 Introduction **4**

2 Parity - Time ($\mathcal{PT}$) Symmetry Theory **5**

3 Theoretical EM Backround **7**
3.1 Maxwell's Equations & EM Wave Propagation 7
3.2 The Dielectric Function of the Free Electron Gas 11
3.3 The Dielectric function in the RPA 13
3.4 The Dispersion of the Free Electron Gas and Volume Plasmons 18

4 Surface Plasmon Polaritons at Metal / Insulator Interfaces **20**
4.1 The Wave Equation 20
4.2 Propagation Geometry 21
4.3 Surface Plasmon Polaritons at a Single Interface 23
4.4 Active Dielectric - PT Gain 29
4.5 Surface Plasmon Polaritons at a Bi-Layer System 33

5 Simulations **39**

6 Conclusion **44**

Abstract

The purpose of this thesis is to examine parity-time surface plasmon polaritons(SPP) known as $\mathcal{PT}$ plasmons, in short, in rectangular geometries. We start by defining what is a $\mathcal{PT}$ symmetry. Then we continue by analyzing the theoretical background of the electromagnetic(EM) waves and the dielectric function in both classical,using the Drude model, and quantum approach, using the random phase approximation(RPA). Furthermore, we examine the dispersion of volume(bulk) plasmons and we move directly to the surface plasmons at single- and multi- layer interfaces, where we find a gain that counterbalance the losses of the physical system and has similar properties as of the $\mathcal{PT}$ symmetry. Finally we perform some simulations using the COMSOL Multiphysics software for those interfaces and for graphene and we present our conclusions.

Chapter 1

Introduction

The study of surface plasmons, which are created when incident light interacts with electrons to create a surface-bound electromagnetic wave, is known as plasmonics. Plasmons are appealing for the development of new technologies with a variety of applications since they can arrange light to nanoscale volumes. Plasmons are mysterious phenomena that have drawn a lot of attention for their capacity to contain and control electromagnetic waves at length scales considerably smaller than the wavelength of light. This skill has enormous potential for use in a wide range of fields, including optics, electronics, biology, and energy harvesting. The basic idea behind plasmonics is the stimulation of surface plasmons, which normally happens when light photons interact with the electrons at a metal-dielectric interface. When electromagnetic surface waves emerge as a result of this interaction, they have the potential to spread over the metal-dielectric border and confine light to nanoscale dimensions. Especially when these EM waves are polarized then we have a surface plasmon polariton (SPP).

Chapter 2

Parity - Time ($\mathcal{PT}$) Symmetry Theory

We define $\hat{T}$ as the *time* reversal operator and $\hat{P}$ as the space reversal operator, known as *parity* operator. If the system obeys T-symmetry, the evolution can be time-reversed, so the system belongs to the same PHASE TRAJECTORY, but we now have $t \to -t$(going backwards).Similarly we have for P-symmetry with $r \to -r$.

These two symmetries can be showed in the following equations:

$$\hat{P}: \ \hat{P}\,|\vec{r},t\rangle = |-\vec{r},t\rangle \tag{2.0.1}$$

$$\hat{T}: \ \hat{T}\,|\vec{r},t\rangle = \langle\vec{r},-t| = |\vec{r},-t\rangle^* \tag{2.0.2}$$

$$\hat{P}\hat{T}: \ \hat{P}\hat{T}\,|\vec{r},t\rangle = |-\vec{r},-t\rangle^* \tag{2.0.3}$$

We can also see the symmetries in the Hamiltonian operator regarding parity, time and parity-time. Thus we have:

$$\hat{P}: \ \hat{H}(\vec{p},\vec{r},t) = \hat{H}(-\vec{p},-\vec{r},t) \tag{2.0.4}$$

$$\hat{T}: \ \hat{H}(\vec{p},\vec{r},t) = \hat{H}^*(-\vec{p},\vec{r},-t) \tag{2.0.5}$$

$$\hat{P}\hat{T}: \ \hat{H}(\vec{p},\vec{r},t) = \hat{H}^*(\vec{p},-\vec{r},-t) \tag{2.0.6}$$

Furthermore, for the $\hat{P}$ operator we also have symmetries for the current $\vec{J}$ and the electric field $\vec{E}$. Those symmetries can be applied for polar vectors where the axial vectors are not affected. Similarly we can see that the magnetic field ,$\vec{H}$, and the angular momentum, $\vec{L}$, are invariant under $\hat{P}$ symmetry.

In general, for both symmetries, we obtain:

$$\hat{P}^\dagger \vec{r} \hat{P} = -\vec{r} \tag{2.0.7}$$

$$\hat{P}^\dagger \vec{p} \hat{P} = -\vec{p} \tag{2.0.8}$$

$$\hat{P}^\dagger \vec{L} \hat{P} = \vec{L} \tag{2.0.9}$$

$$\hat{T}^\dagger \vec{r} \hat{T} = \vec{r} \tag{2.0.10}$$

$$\hat{T}^\dagger \vec{p} \hat{T} = -\vec{p} \tag{2.0.11}$$

$$\hat{T}^\dagger \vec{L} \hat{T} = -\vec{L} \tag{2.0.12}$$

We also define the symmetric operator, $\hat{O}$, that gives the following permutation:

$$[\hat{H}, \hat{O}] = 0 \tag{2.0.13}$$

Thus we can see that PT-symmetric Hamiltonians have a real eigen-value spectrum ω_k, in their PT-symmetric phase, when the corresponding eigen-solutions ψ_k, satisfy PT symmetry.

$$\hat{P}\hat{T} \left|\vec{r}, t\right\rangle = \left|-\vec{r}, -t\right\rangle^* = \left|\vec{r}, t\right\rangle \Rightarrow [\hat{H}, \hat{P}\hat{T}] = 0 \tag{2.0.14}$$

From (2.0.14) we can see that the system has a real energy spectrum[1][7].

Chapter 3

Theoretical EM Backround

3.1 Maxwell's Equations & EM Wave Propagation

A solid comprehension of how metals react to electromagnetic fields can be achieved using the principles outlined in Maxwell's equations within a classical limit. This applies also to metallic nanostructures with size of a few nanometers, eliminating the necessity to rely on quantum mechanics. This is due to the abundant presence of free carriers in metals, leading to extremely close spacings between electron energy levels in comparison to the thermal energy excitations at room temperature, which are on the order of $k_B T$.

We take as a starting point Maxwell's equations of macroscopic electromagnetism in the following form:

$$\nabla \cdot \boldsymbol{D} = \rho_{ext} \tag{3.1.1}$$

$$\nabla \cdot \boldsymbol{B} = 0 \tag{3.1.2}$$

$$\nabla \times \boldsymbol{E} = -\frac{\partial \boldsymbol{B}}{\partial t} \tag{3.1.3}$$

$$\nabla \times \boldsymbol{H} = \boldsymbol{J}_{ext} + \frac{\partial \boldsymbol{D}}{\partial t} \tag{3.1.4}$$

We differentiate between the charge and current densities originating from external sources $(\rho_{ext}, \boldsymbol{J_{ext}})$ and those that exist internally within the system $(\rho, \boldsymbol{J})$. Consequently, the total charge density is given by $\rho_{tot} = \rho_{ext} + \rho$, and the total current density by $\boldsymbol{J_{tot}} = \boldsymbol{J_{ext}} + \boldsymbol{J}$. The external charge and current densities act as driving forces for the system, while the internal ones react and adapt in response to the external stimuli.

The interconnection between the four macroscopic fields is established through the polarization

P and magnetization M, which serve as additional links. Thus we have:

$$\boldsymbol{D} = \epsilon_0 \boldsymbol{E} + \boldsymbol{P} \tag{3.1.5}$$

$$\boldsymbol{H} = \frac{1}{\mu_0}\boldsymbol{B} - \boldsymbol{M} \tag{3.1.6}$$

where ε_0 and μ_0 are the electric permittivity[1] and magnetic permeability[2] of vacuum, respectively.

$\boldsymbol{P}$ represents the electric dipole moment per unit volume within the material, resulting from the alignment of microscopic dipoles in response to the electric field. It is connected to the internal charge density through the following relationship:

$$\begin{cases} \nabla \cdot \boldsymbol{P} = -\rho \\ \nabla \cdot \boldsymbol{J} = -\dfrac{\partial \rho}{\partial t} \end{cases} \Rightarrow \boldsymbol{J} = \frac{\partial \boldsymbol{P}}{\partial t} \tag{3.1.7}$$

The equation $\nabla \cdot \boldsymbol{J} = -\dfrac{\partial \rho}{\partial t}$ is known as the continuity equation.

Now if we combine eq.(3.1.1) and eq.(3.1.5) we obtain the following:

$$\nabla \cdot \boldsymbol{E} = \frac{\rho_{ext}}{\epsilon_0} \tag{3.1.8}$$

We can stop to the linear response, isotropic and nonmagnetic media, we find the following results:

$$\boldsymbol{D} = \epsilon_0 \epsilon \boldsymbol{E} \tag{3.1.9}$$

$$\boldsymbol{B} = \mu_0 \mu \boldsymbol{H} \tag{3.1.10}$$

where ϵ and μ are the dielectric constant and relative permeability, respectively. To our case we can define $\mu = 1$. The linear correlation Eq.(3.1.9) between $\boldsymbol{D}$ and $\boldsymbol{E}$ is frequently expressed implicitly by incorporating the dielectric susceptibility χ, which describes the linear relationship between $\boldsymbol{P}$ and $\boldsymbol{E}$ via

$$\boldsymbol{P} = \epsilon_0 \chi \boldsymbol{E}, \quad \epsilon = 1 + \chi \tag{3.1.11}$$

[1] $\epsilon_0 \simeq 8.854 \times 10^{-12} F/m$
[2] $\mu_0 \simeq 1.257 \times 10^{-6} H/m$

Another significant constitutive linear relationship to mention is the connection between the internal current density $\boldsymbol{J}$ and the electric field $\boldsymbol{E}$, which is defined by the conductivity σ:

$$\boldsymbol{J} = \sigma \boldsymbol{E} \tag{3.1.12}$$

Now we will demonstrate the close connection between ϵ and σ, showing that electromagnetic phenomena involving metals can indeed be explained using either quantity. However, it is important to note that Eqs. (3.1.9) and (3.1.12) are only applicable to linear materials that do not exhibit temporal or spatial dispersion. Since the optical behavior of metals is clearly affected by the frequency (and possibly the wave vector) of the EM wave, we must consider the non-local effects in time and space. As a result, we generalize the linear relationships to encompass $\epsilon_0\epsilon$ and σ, which accurately describe the impulse response of the corresponding linear relationship.

For a local response, the functional form of the impulse response functions is similar of a δ-function and they are given below:

$$\mathbf{D}(\mathbf{r}, t) = \epsilon_0 \int dt' d\mathbf{r}' \epsilon(\mathbf{r}-\mathbf{r}', t-t')\mathbf{E}(\mathbf{r}', t') \tag{3.1.13}$$

$$\mathbf{J}(\mathbf{r}, t) = \int dt' d\mathbf{r}' \sigma(\mathbf{r}-\mathbf{r}', t-t')\mathbf{E}(\mathbf{r}', t') \tag{3.1.14}$$

Applying Fourier Transform in Eqs. (3.1.13) and (3.1.14), we decompose the fields into individual plane-wave components of wave vector $\mathbf{K}$ and angular frequency ω. This leads to the constitutive relation in the Fourier Domain:

$$\mathbf{D}(\mathbf{K}, \omega) = \epsilon_0 \epsilon(\mathbf{K}, \omega)\mathbf{E}(\mathbf{K}, \omega) \tag{3.1.15}$$

$$\mathbf{J}(\mathbf{K}, \omega) = \sigma(\mathbf{K}, \omega)\mathbf{E}(\mathbf{K}, \omega) \tag{3.1.16}$$

Using Eqs. (3.1.5),(3.1.6), (3.1.15), (3.1.16) we finally obtain the relation of the dielectric function and the conductivity, given by:

$$\epsilon(\mathbf{K}, \omega) = 1 + \frac{i\sigma(\mathbf{K}, \omega)}{\epsilon_0 \omega} \tag{3.1.17}$$

In the interaction of light with metals, the general form of the dielectric response $\epsilon(\mathbf{K}, \omega)$ can be simplified to the limit of a spatially local response via $\epsilon(\mathbf{K} = \mathbf{0}, \omega) = \epsilon(\omega)$. The simplification is true as long as all of the characteristic parameters, such as the size of the unit cell or the mean free path of the electrons, are significantly shorter than the wavelength λ in the material. Generally speaking, this is still met at UV frequencies.

In general we know that $\epsilon(\omega) = \epsilon_1(\omega) + \epsilon_2(\omega)$, where $\epsilon_1(\omega)$ and $\epsilon_2(\omega)$ are the real and imaginary parts of the dielectric function $\epsilon(\omega)$, and $\sigma(\omega) = \sigma_1(\omega) + \sigma_2(\omega)$,in which are complex valid functions of angular frequency ω, linked via Eq. (3.1.17). At optical frequencies, ϵ can be experimentally determined for example via reflectivity studies and the determination of the complex refractive index $\tilde{n}(\omega) = n(\omega) + i\kappa(\omega)$ of the medium, defined as $\tilde{n} = \sqrt{\epsilon}$. Explicitly, this yields to some basic complex algebra obtaining the following results:

$$\epsilon_1 = n^2 - \kappa^2 \tag{3.1.18}$$

$$\epsilon_2 = 2n\kappa \tag{3.1.19}$$

$$n^2 = \frac{1}{2}\left(\epsilon_1 + \sqrt{\epsilon_1^2 + \epsilon_2^2}\right) \tag{3.1.20}$$

$$\kappa = \frac{\epsilon_2}{2n} \tag{3.1.21}$$

where κ is called the extinction coefficient and determines the optical absorption of electromagnetic waves propagating through the medium. It is linked to the absorption coefficient α of Beer's law(the intenisty of a beam propagating through the medium $I(x) = I_0 \exp(-\alpha x)$) by the relation

$$\alpha(\omega) = \frac{2\kappa(\omega)\omega}{c} \tag{3.1.22}$$

Therefore we see that the imaginary part ϵ_2 of the dielectric function determines the amount of absorption inside the medium. For $|\epsilon_1| \gg |\epsilon_2|$, the real part n of the refractive index, quantifying the lowering of the phase velocity, v_{ph}, of the propagating waves due to polarization of the material, is mainly determined by ϵ_1. By examining Eq. (3.1.17), we see that the real part of σ determines the amount of absorption, while the imaginary part contributes to ϵ_1 and therefore to the amount of polarization.

We now examine the traveling - wave solution of Maxwell's equations in the absence of external stimuli. Combining the curl Eqs. (3.1.3), (3.1.4)

$$\nabla \times \nabla \times \mathbf{E} = -\mu_0 \frac{\partial^2 \mathbf{D}}{\partial t^2} \tag{3.1.23}$$

which leads to the wave solution

$$\mathbf{K(K \cdot E)} - K^2\mathbf{E} = -\epsilon(\mathbf{K}, \omega)\frac{\omega^2}{c^2}\mathbf{E} \tag{3.1.24}$$

in the time and Fourier domains, respectively. Two cases need to be distinguished, depending on the polarization direction of the electric field vector. We look first for transverse waves, where

$\mathbf{K}\cdot\mathbf{E} = 0$, yielding to the generic dispersion relation

$$K^2 = \epsilon(\mathbf{K}, \omega)\frac{\omega^2}{c^2} \tag{3.1.25}$$

For longitudinal waves, the second case, we have that $\epsilon(\mathbf{K}, \omega) = 0$, signifying that longitudinal collective oscillations can only occur at frequencies corresponding to zeros of $\epsilon(\omega)$.

3.2 The Dielectric Function of the Free Electron Gas

In this section, we study the dielectric function that we are going to use in this thesis. We can write a simple equation of motion for an electron of the plasma sea subjected to an external electric field $\boldsymbol{E}$:

$$m\ddot{x} + m\gamma\dot{x} = -e\boldsymbol{E} \tag{3.2.1}$$

where m is the electron mass of the plasma, and γ are the losses. We assume a harmonic time dependence $\boldsymbol{E}(t) = \boldsymbol{E}_0 e^{-i\omega t}$ of the driving field. Therefore a particular solution of this equation describing the oscillation of the electron is $\boldsymbol{x}(t) = \boldsymbol{x}_0 e^{-i\omega t}$, where $\boldsymbol{x}_0$ is the initial spacial parameter for $t = 0$, and $\dfrac{\partial}{\partial t} \to -i\omega$. Thus, we have:

$$-m\omega^2\boldsymbol{x}_0 - im\gamma\omega\boldsymbol{x}_0 = -e\boldsymbol{E}_0 \tag{3.2.2}$$

which gives us the following relation between x_0 and $\boldsymbol{E}_0$:

$$\boldsymbol{x}_0 = \frac{e}{m(\omega^2 + i\gamma\omega)}\boldsymbol{E}_0 \tag{3.2.3}$$

and when we evolve it through time we obtain:

$$\boldsymbol{x}(t) = \frac{e}{m(\omega^2 + i\gamma\omega)}\boldsymbol{E}(t) \tag{3.2.4}$$

The displaced electrons contribute to the macroscopic polarization $\boldsymbol{P} = -ne\boldsymbol{x}$, explicitly given by:

$$\boldsymbol{P} = -\frac{ne^2}{m(\omega^2 + i\gamma\omega)}\boldsymbol{E} \tag{3.2.5}$$

Thus we obtain for the electric displacement field we have:

$$\boldsymbol{D} = \epsilon_0(1 - \frac{\omega_p^2}{\omega^2 + i\gamma\omega})\boldsymbol{E} \tag{3.2.6}$$

where $\omega_p^2 = \dfrac{ne^2}{\epsilon_0 m}$ is the plasma frequency of the free electron gas. Thus the dielectric function of the free electron gas is given by:

$$\epsilon(\omega) = 1 - \frac{\omega_p^2}{\omega^2 + i\gamma\omega} \tag{3.2.7}$$

The real and imaginary parts of this complex dielectric function $\epsilon(\omega) = \epsilon_{r,m}(\omega) + i\epsilon_{i,m}(\omega)$ are given by the following :

$$\epsilon_{r,m}(\omega) = 1 - \frac{\omega_p^2}{\omega^2 + \gamma^2} \tag{3.2.8}$$

$$\epsilon_{i,m}(\omega) = \frac{\omega_p^2}{\omega(\gamma + \omega^2\gamma^2)} \tag{3.2.9}$$

In this context, we will focus only on frequencies ω that are lower than ω_p, where metals exhibit their typical metallic behavior. When dealing with high frequencies near ω_p, the value of $\omega\tau \gg 1$, resulting in minimal damping. In this case, the majority of $\epsilon(\omega)$ is characterized by being primarily a real value:

$$\epsilon(\omega) = 1 - \frac{\omega_p^2}{\omega^2} \tag{3.2.10}$$

can be taken as the dielectric function of the undamped free electron plasma.

Next we study the regime of very low frequencies, where $\omega\tau \ll 1$. Therefore, we have that $\epsilon_{i,m} \gg \epsilon_{r,m}$, and both the real and the imaginary part of this complex refractive index have a similar magnitude given by the following equation

$$n \approx \kappa = \sqrt{\frac{\epsilon_{i,m}}{2}} = \sqrt{\frac{\tau\omega_p^2}{2\omega}} \tag{3.2.11}$$

In this region, metals are mostly absorbing, with an absorption coefficient α given by:

$$\alpha = \sqrt{\frac{2\omega_p^2\tau\omega}{c^2}} \tag{3.2.12}$$

By introducing the conductivity σ_0 of the system, this expression can be re-written using $\sigma_0 = \frac{ne^2\tau}{m} = \omega_p^2\tau\epsilon_0$ to

$$\alpha = \sqrt{2\sigma_0\omega\mu_0} \tag{3.2.13}$$

The application of Beer's law of absorption suggests that for low frequencies the fields fall off inside the metal as $\exp(-z/\delta)$, where δ is the skin depth

$$\delta = \frac{2}{\alpha} = \frac{c}{\kappa\omega} = \sqrt{\frac{2}{\sigma_0\omega\mu_0}} \tag{3.2.14}$$

This is one of one of many free-electron models. In general we can see that the residual polarization due to the positive backround of the ion cores can be described by adding the term $\mathbf{P}_\infty = \epsilon_0(\epsilon_\infty - 1)\mathbf{E}$, where $\mathbf{P}$ now represents soely the polarization due to free electrons. This effect is therefore described by a dielectric constant ϵ_∞(usually $1 \leq \epsilon_\infty \leq 10$), and we can write the new dielectic function as

$$\epsilon(\omega) = \epsilon_\infty - \frac{\omega_p^2}{\omega^2 + i\gamma\omega} \tag{3.2.15}$$

3.3 The Dielectric function in the RPA

Further investigation of the dynamical dielectric function can be performed using quantum mechanics. An explicit form of $\epsilon(k,\omega)$ including screening effect has been evaluated in the context of the random phase approximation(RPA) as in the electron gas[12]. The hamiltonian, $\hat{H}$, of this system is given by

$$\hat{H} = \sum_{\boldsymbol{k},\sigma} \varepsilon_{\boldsymbol{k}} \alpha^\dagger_{\boldsymbol{k}\sigma}\alpha_{\boldsymbol{k}\sigma} + \frac{1}{2V}\sum_{\boldsymbol{k},\boldsymbol{k'},\boldsymbol{q},\sigma\sigma'} v(\boldsymbol{q})\alpha^\dagger_{\boldsymbol{k}+\boldsymbol{q},\sigma}\alpha^\dagger_{\boldsymbol{k'}-\boldsymbol{q},\sigma'}\alpha_{\boldsymbol{k'}\sigma'}\alpha_{\boldsymbol{k}\sigma} \tag{3.3.1}$$

where the creation,$\alpha^\dagger_{\boldsymbol{k},\sigma}$, and annihilation, $\alpha_{\boldsymbol{k},\sigma}$, operators of the plane waves are connected through the following relation,

$$[\alpha_{\boldsymbol{k}\sigma}, \alpha^\dagger_{\boldsymbol{k'}\sigma'}]_{-\zeta} = \delta_{\boldsymbol{k},\boldsymbol{k'}}\delta_{\sigma,\sigma'}, \;\; \zeta = -1 \tag{3.3.2}$$

where ζ is the symbol of which type of particles we have in our system. For bosons we have that $\zeta = +1$ and for fermions $\zeta = -1$. Here because we are dealing with plasma oscillation systems, we have electrons, hence $\zeta = -1$. The Coulomb potential is defined as:

$$v(\boldsymbol{q}) = \begin{cases} \dfrac{4\pi e^2}{|\boldsymbol{q}|^2}, & \boldsymbol{q} \neq 0 \\ \\ 0, & \boldsymbol{q} = 0 \end{cases} \tag{3.3.3}$$

From the linear response theory we have

$$\frac{1}{\epsilon(\mathbf{q},\omega)} = 1 + \frac{v(\mathbf{q})}{V} \ll \rho_{\mathbf{q}}; \rho^{\dagger}_{\mathbf{q}} \gg^{r}_{\omega} \tag{3.3.4}$$

where $\ll \rho_{\mathbf{q}}; \rho^{\dagger}_{\mathbf{q}} \gg^{r}_{\omega}$ is the retarded Green function density-density with

$$\rho_{\mathbf{q}} = \int d^3x e^{-i\mathbf{q}\cdot\mathbf{x}} \rho(\mathbf{x}) = \sum_{\mathbf{k},\sigma} \alpha^{\dagger}_{\mathbf{k},\sigma} \alpha_{\mathbf{k}\,+\,\mathbf{q},\sigma} \tag{3.3.5}$$

Using the above equations we can now write the Green function of density-density as follows

$$\begin{aligned} \Pi(\mathbf{q},z) = \frac{1}{V} \ll \rho_{\mathbf{q}}; \rho^{\dagger}_{\mathbf{q}} \gg_z &= \frac{1}{V} \sum_{\mathbf{k},\sigma} \ll \alpha^{\dagger}_{\mathbf{k}\sigma} \alpha_{\mathbf{k+q}\sigma}; \rho^{\dagger}_{\mathbf{q}} \gg_z \\ &= \frac{1}{V} \sum_{\mathbf{k},\mathbf{k'},\sigma,\sigma'} \ll \alpha^{\dagger}_{\mathbf{k}\sigma} \alpha_{\mathbf{k+q}\sigma}; \alpha^{\dagger}_{\mathbf{k'+q},\sigma'} \alpha_{\mathbf{k'}\sigma'} \gg_z \end{aligned} \tag{3.3.6}$$

We see that $\Pi(\mathbf{q},z)$ has the form of a particle-hole Green function. Thus we can obtain the following equation of motion

$$z \ll \alpha^{\dagger}_{\mathbf{k}\sigma} \alpha_{\mathbf{k+q},\sigma}; \rho^{\dagger}_{\mathbf{q}} \gg_z = \left\langle [\alpha^{\dagger}_{\mathbf{k}\sigma} \alpha_{\mathbf{k+q},\sigma}; \rho^{\dagger}_{\mathbf{q}}] \right\rangle + \ll [\alpha^{\dagger}_{\mathbf{k}\sigma} \alpha_{\mathbf{k+q},\sigma}, H - \mu\hat{N}]; \rho^{\dagger}_{\mathbf{q}} \gg_z \tag{3.3.7}$$

where $\hat{N} = \sum_{\mathbf{k},\sigma} \alpha^{\dagger}_{\mathbf{k}\sigma} \alpha_{\mathbf{k}\sigma}$ is the particle number operator and μ is the chemical potential of the system.

The final form of the equation of motion is

$$\begin{aligned} [z - (\varepsilon_{\mathbf{k+q}} - \varepsilon_{\mathbf{k}})] \ll \alpha^{\dagger}_{\mathbf{k}\sigma} \alpha_{\mathbf{k+q},\sigma}; \rho^{\dagger}_{\mathbf{q}} \gg_z &= \left[\left\langle \alpha^{\dagger}_{\mathbf{k}\sigma} \alpha_{\mathbf{k}\sigma} \right\rangle - \left\langle \alpha^{\dagger}_{\mathbf{k+q},\sigma} \alpha_{\mathbf{k+q},\sigma} \right\rangle \right] \\ &+ \frac{1}{V} \sum_{\mathbf{k'},\mathbf{q'},\sigma'} v(\mathbf{q'}) \ll \alpha^{\dagger}_{\mathbf{k}\sigma} \alpha^{\dagger}_{\mathbf{k'+q'},\sigma'} \alpha_{\mathbf{k'}\sigma'} \alpha_{\mathbf{k+q+q'},\sigma'}; \rho^{\dagger}_{\mathbf{q}} \gg_z \\ &- \frac{1}{V} \sum_{\mathbf{k'},\mathbf{q'},\sigma'} v(\mathbf{q'}) \ll \alpha^{\dagger}_{\mathbf{k+q'},\sigma} \alpha^{\dagger}_{\mathbf{k'-q'},\sigma'} \alpha_{\mathbf{k'}\sigma'} \alpha_{\mathbf{k+q},\sigma}; \rho_{\mathbf{q}} \gg_z \end{aligned} \tag{3.3.8}$$

We can see that two new Green functions appeared. We can solve this system by applying the Hartree-Fock approximation:

$$\begin{aligned}\ll \alpha^\dagger_{\lambda_1}\alpha^\dagger_{\lambda_2}\alpha_{\lambda_3}\alpha_{\lambda_4};\alpha^\dagger_\nu\alpha_\nu \gg_z \simeq\ & \langle\alpha^\dagger_{\lambda_2}\alpha_{\lambda_3}\rangle \ll \alpha^\dagger_{\lambda_1}\alpha_{\lambda_4};\alpha^\dagger_\nu\alpha_{\nu'} \gg_z \\ &+\zeta\langle\alpha^\dagger_{\lambda_1}\alpha_{\lambda_3}\rangle \ll \alpha^\dagger_{\lambda_2}\alpha_{\lambda_4};\alpha^\dagger_\nu\alpha_{\nu'} \gg_z \\ &+\zeta\langle\alpha^\dagger_{\lambda_2}\alpha_{\lambda_4}\rangle \ll \alpha^\dagger_{\lambda_1}\alpha_{\lambda_3};\alpha^\dagger_\nu\alpha_{\nu'} \gg_z \\ &+\langle\alpha^\dagger_{\lambda_1}\alpha_{\lambda_4}\rangle \ll \alpha^\dagger_{\lambda_2}\alpha_{\lambda_3};\alpha^\dagger_\nu\alpha_{\nu'} \gg_z \end{aligned} \tag{3.3.9}$$

Using the identity

$$\langle\alpha^\dagger_{\mathbf{k}\sigma}\alpha_{\mathbf{k}'\sigma'}\rangle = \delta_{\sigma\sigma'}\delta_{\mathbf{k}\mathbf{k}'}\langle\alpha^\dagger_{\mathbf{k}\sigma}\alpha_{\mathbf{k}\sigma}\rangle \tag{3.3.10}$$

in the random phase approximation, the equation of motion has the following form

$$\begin{aligned}[z-(E_{\mathbf{k}+\mathbf{q},\sigma}-E_{\mathbf{k}\sigma})] \ll \alpha^\dagger_{\mathbf{k}\sigma}\alpha_{\mathbf{k}+\mathbf{q},\sigma};\rho^\dagger_{\mathbf{q}} \gg_z =& \left[\langle\alpha^\dagger_{\mathbf{k}\sigma}\alpha_{\mathbf{k}\sigma}\rangle - \langle\alpha^\dagger_{\mathbf{k}+\mathbf{q},\sigma}\alpha_{\mathbf{k}+\mathbf{q},\sigma}\rangle\right] \\ \times\left[1+\frac{v(\mathbf{q})}{V}\ll\rho_{\mathbf{q}};\rho^\dagger_{\mathbf{q}}\gg_z - \frac{1}{V}\sum_{\mathbf{k}'}v(\mathbf{k}-\mathbf{k}')\ll\alpha^\dagger_{\mathbf{k}'\sigma}\alpha_{\mathbf{k}'+\mathbf{q},\sigma};\rho^\dagger_{\mathbf{q}}\gg_z\right]\end{aligned} \tag{3.3.11}$$

where

$$E_{\mathbf{k}\sigma} = \varepsilon_{\mathbf{k}} + \frac{1}{V}\sum_{\mathbf{k}',\sigma'}\langle\alpha^\dagger_{\mathbf{k}'\sigma'}\alpha_{\mathbf{k}'\sigma'}\rangle[v(0)-\delta_{\sigma\sigma'}v(\mathbf{k}-\mathbf{k}')] \tag{3.3.12}$$

The term $v(\mathbf{q})$ is called direct term and $v(\mathbf{k}-\mathbf{k}')$ is called exchange term. For small wavevectors, $\mathbf{q}\to 0$ we have that $v(\mathbf{q}) = 4\pi e^2/|\mathbf{q}|^2 \to \infty$. Therefore we expect the direct term to have the dominant role over the exchange term. Thus, we have that

$$\langle\alpha^\dagger_{\mathbf{k}\sigma}\alpha_{\mathbf{k}\sigma}\rangle \approx f(\varepsilon_{\mathbf{k}}) = \frac{1}{e^{\beta(\varepsilon_{\mathbf{k}}-\mu)}+1} \tag{3.3.13}$$

where $f(\varepsilon)$ is the Fermi-Dirac distribution function, $\beta = 1/k_BT$ with Boltzmann's constant denoted by k_B and T is the absolute temperature. Ignoring the exchange term the Green function takes the following form

$$\ll \alpha^\dagger_{\mathbf{k}\sigma}\alpha_{\mathbf{k}+\mathbf{q},\sigma};\rho^\dagger_{\mathbf{q}}\gg_z = -\frac{f(\varepsilon_{\mathbf{k}+\mathbf{q}})-f(\varepsilon_{\mathbf{k}})}{z-(\varepsilon_{\mathbf{k}+\mathbf{q}}-\varepsilon_{\mathbf{k}})}\left[1+\frac{v(\mathbf{q})}{V}\ll\rho_{\mathbf{q}};\rho^\dagger_{\mathbf{q}}\gg_z\right] \tag{3.3.14}$$

At zero temperature, the chemical potential is equal to the Fermi energy, i.e., $\mu = E_F$ and the Fermi-Dirac distribution is reduced to Heaviside step function, thus, $f(\varepsilon_{\mathbf{k}})|_{T=0} = \theta(E_F - \varepsilon_{\mathbf{k}})$. The kinetic energy of each electron of mass m in state $\mathbf{k}$ is given by

$$\varepsilon_{\mathbf{k}} = \frac{\hbar^2 \mathbf{k}^2}{2m}, \tag{3.3.15}$$

hence

$$\varepsilon_{\mathbf{k+q}} - \varepsilon_{\mathbf{k}} = \frac{1}{2m}(|\mathbf{q}|^2 + 2\mathbf{k}\cdot\mathbf{q}) \tag{3.3.16}$$

where $\hbar = 1$.

Summing the left and right part of the above equation over $(\mathbf{k}, \sigma)$ we obtain the final Green function of density-density in the RPA is

$$\Pi_{RPA}(\mathbf{q}, z) = \frac{1}{V} \ll \rho_{\mathbf{q}}; \rho_{\mathbf{q}}^{\dagger} \gg_z^{RPA} = \frac{\Pi_0(\mathbf{q}, z)}{1 - v(\mathbf{q})\Pi_0(\mathbf{q}, z)} \tag{3.3.17}$$

where

$$\Pi_0(\mathbf{q}, z) \equiv \frac{1}{V} \ll \rho_{\mathbf{q}}; \rho_{\mathbf{q}}^{\dagger} \gg_z^{(0)} = -\frac{2}{V} \sum_{\mathbf{k}} \frac{f(\varepsilon_{\mathbf{k+q}}) - f(\varepsilon_{\mathbf{k}})}{z - (\varepsilon_{\mathbf{k+q}} - \varepsilon_{\mathbf{k}})} \tag{3.3.18}$$

is called Lindhard function[12]. We can easily see that the Green function of density-density of the non-interacting electrons equally related to $\Pi_0(\mathbf{q}, z)$. Substituting $z = \omega + i\eta$ we obtain the dielectric function in the RPA approximation

$$\epsilon_{RPA}(\mathbf{q}, \omega) = 1 - v(\mathbf{q})\Pi_0(\mathbf{q}, \omega + i\eta) = 1 + \frac{2v(\mathbf{q})}{V} \sum_{\mathbf{k}} \frac{f(\varepsilon_{\mathbf{k+q}}) - f(\varepsilon_{\mathbf{k}})}{\omega - (\varepsilon_{\mathbf{k+q}} - \varepsilon_{\mathbf{k}}) + i\eta} \tag{3.3.19}$$

By setting $\mathbf{k} + \mathbf{q} \to -\mathbf{k}$ and we re-write the Lindhard function as follows

$$\begin{aligned} \Pi_0(\mathbf{q}, z) &= \frac{2}{V} \sum_{\mathbf{k}} f(\varepsilon_{\mathbf{k}}) \left[\frac{1}{z - (\varepsilon_{\mathbf{k+q}} - \varepsilon_{\mathbf{k}})} - \frac{1}{z + (\varepsilon_{\mathbf{k+q}} - \varepsilon_{\mathbf{k}})} \right] \\ &= \frac{4}{V} \sum_{\mathbf{k}} f(\varepsilon_{\mathbf{k}})[1 - f(\varepsilon_{\mathbf{k+q}})] \frac{\varepsilon_{\mathbf{k+q}} - \varepsilon_{\mathbf{k}}}{z^2 - (\varepsilon_{\mathbf{k+q}} - \varepsilon_{\mathbf{k}})^2} \end{aligned} \tag{3.3.20}$$

At zero temperature, due to the Heaviside step function, the surviving terms in the summation above are those with $\mathbf{k} < k_F$, where k_F is the Fermi wavenumber and related to the Fermi energy as $k_F = (2mE_F)^{1/2}$. Thus, we have

$$\begin{aligned}\Pi_0(\mathbf{q}, z) &= \frac{2}{V} \sum_{|\mathbf{k}|<k_F} \left[\frac{1}{z - (\varepsilon_{\mathbf{k}+\mathbf{q}} - \varepsilon_{\mathbf{k}})} - \frac{1}{z + (\varepsilon_{\mathbf{k}+\mathbf{q}} - \varepsilon_{\mathbf{k}})} \right] \\ &= \frac{4}{V} \sum_{\substack{|\mathbf{k}|<k_F \\ |\mathbf{k}+\mathbf{q}|>k_F}} \frac{\varepsilon_{\mathbf{k}+\mathbf{q}} - \varepsilon_{\mathbf{k}}}{z^2 - (\varepsilon_{\mathbf{k}+\mathbf{q}} - \varepsilon_{\mathbf{k}})^2}, \quad T = 0 \end{aligned} \tag{3.3.21}$$

Summation turns into integration by using the formula $V^{-1} \sum_{\mathbf{k}}(...) \to (2\pi)^{-3} \int d^3k(...)$, hence

$$\Pi_0(\mathbf{q}, \omega) = \frac{4}{(2\pi)^3} \int d^3k \frac{\varepsilon_{\mathbf{k}+\mathbf{q}} - \varepsilon_{\mathbf{k}}}{z^2 - (\varepsilon_{\mathbf{k}+\mathbf{q}} - \varepsilon_{\mathbf{k}})^2} \tag{3.3.22}$$

As we mentioned before, the imaginary part in z guarantees the convergence around the poles $\omega = \pm(\varepsilon_{\mathbf{k}+\mathbf{q}} - \varepsilon_{\mathbf{k}})$. The poles of Π_0 determine the Landau-damping regime where plasmons decay into electron-hole pairs excitation. In particular, the damping regime is a continuum bounded by the limit values of $(\varepsilon_{\mathbf{k}+\mathbf{q}} - \varepsilon_{\mathbf{k}})$; $\mathbf{k}$ takes the maximum absolute value $|\mathbf{k}| = k_F$ and the inner product $k_F \hat{\mathbf{k}} \cdot \mathbf{q} = \pm k_F |\mathbf{q}|$.

Thus the Landau damping continuum will be under the following condition

$$\frac{|\mathbf{q}|}{2m}(|\mathbf{q}| - 2k_F) < \omega < \frac{|\mathbf{q}|}{2m}(|\mathbf{q}| + 2k_F) \tag{3.3.23}$$

In RPA approach, the conductivity reads as

$$\sigma = \frac{i\omega e^2}{q^2} \Pi_0(\mathbf{q}, \omega) \tag{3.3.24}$$

Now we can reveal the relation betweeen the dielectric function and conductivity as follows

$$\epsilon_{RPA}(\mathbf{q}, \omega) = 1 + i \frac{q^2 v(\mathbf{q})}{\omega e^2} \sigma(\mathbf{q}, \omega) \tag{3.3.25}$$

with $v(\mathbf{q})$ being the Coulomb potential as follows

$$v(\mathbf{q}) = \begin{cases} 0, \ \ \mathbf{q} = 0 \\ \dfrac{2\pi e^2}{|\mathbf{q}|^2 \varepsilon_b}, \ \ (2D) \\ \dfrac{4\pi e^2}{|\mathbf{q}|^2 \varepsilon_b}, \ \ (3D) \end{cases} \tag{3.3.26}$$

where ε_b represents the background lattice dielectric constant of the system.

Changing to spherical coordinates (r, θ, φ), where $r = |\mathbf{k}|$ and θ are the angle between $\mathbf{k}$ and $\mathbf{q}$, we obtain the following

$$\Pi_0(\mathbf{q}, \omega) = \frac{2k_F^4|\mathbf{q}|}{(2\pi)^3 m z^2} \int_0^{2\pi} d\phi \int_0^1 dx\, x^2 \int_0^{\pi} d\theta \frac{(\frac{|\mathbf{q}|}{k_F} + 2x\cos\theta)\sin\theta}{1 - (\frac{v_F|\mathbf{q}|}{z})^2 (\frac{|\mathbf{q}|}{2k_F} + x\cos\theta)^2} \tag{3.3.27}$$

where $x = r/k_F$ is a dimensionless variable and $v_F = k_F/m$ the Fermi velocity. In the non-static($\omega \gg v_F|\mathbf{q}|$) and long wavelength($|\mathbf{q}| \ll k_F$) limits we can expand the above integral in a power of series of $|\mathbf{q}|$. We keep up to $|\mathbf{q}|^3$ orders and we keep the imaginary part of z zero, that is $z = \omega$. That leads to a third-order approximation polarizability function which is

$$\Pi_0(|\mathbf{q}|, \omega) = \frac{k_F^3|\mathbf{q}|^2}{3\pi^2 m\omega^2}\left(1 + \frac{3v_F^2|\mathbf{q}|^2}{5\omega^2}\right) \tag{3.3.28}$$

Using the 3D formula for the Coulomb interaction we have that

$$\epsilon(|\mathbf{q}| \to 0, \omega) = 1 - \frac{\omega_p(0)^2}{\omega^2}\left(1 + \frac{3}{5}\left(\frac{v_F|\mathbf{q}|}{\omega}\right)^2\right) \tag{3.3.29}$$

where the vacuum here is assumed as the background ($\varepsilon_b = 1$).

The plasmon condition determines the q- dependent plasmon dispersion relation $\omega_p(q)$. Demanding $\epsilon(q, \omega) = 0$ the above equation yields approximately to

$$\omega_p(q) \approx \omega_p(0)\left(1 + \frac{3}{10}\left(\frac{v_F|\mathbf{q}|}{\omega}\right)^2\right) \tag{3.3.30}$$

where $q = |\mathbf{q}|$. If we set $q = 0$, we get the Drude dielectric function $\epsilon(q, \omega)$.

We can easily see that $3D$ plasmons are purely classical modes as they do not include any quantum quantity, such as v_F, which appears as non-local correction in sub-leading terms.

3.4 The Dispersion of the Free Electron Gas and Volume Plasmons

Now we study the $\omega > \omega_p$ regime of the free electron gas model. Using the dispersion relation for the transverse wave we conclude to

$$\omega^2 = \omega_p^2 + \beta^2 c^2 \tag{3.4.1}$$

This relation is for a generic free electron metal. The propagation of transverse electromagnetic waves only exists in the $\omega > \omega_p$ domain and the plasma supports transverse wave propagating with a group velocity $v_g = d\omega/d\beta < c$.

In Fig.3.1, we present the dispersion relation of a bulk plasmon

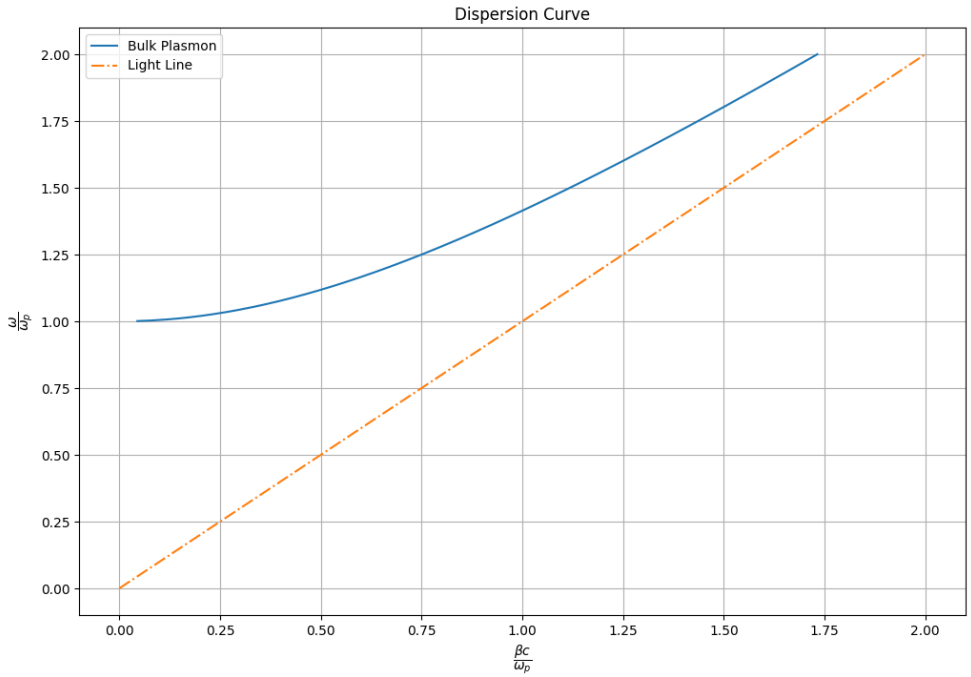

Figure 3.1: The dispersion relation $\omega - \beta$ of a bulk plasmon. Both ω and β are normalized.

Chapter 4

Surface Plasmon Polaritons at Metal / Insulator Interfaces

4.1 The Wave Equation

From the four Maxwell Equations inside media, combining Eqs.(3.1.3) and (3.1.4) we have:

$$\nabla \times \nabla \times \boldsymbol{E} = -\mu_0 \frac{\partial^2 \boldsymbol{D}}{\partial t^2} \tag{4.1.1}$$

Now by using the identities

$$\begin{cases} \nabla \times \nabla \times \boldsymbol{E} = \nabla(\nabla \cdot \boldsymbol{E}) - \nabla^2 \boldsymbol{E} \\ \nabla \cdot (\epsilon \boldsymbol{E}) = \boldsymbol{E} \cdot \nabla \epsilon + \epsilon \nabla \cdot \boldsymbol{E} \end{cases} \tag{4.1.2}$$

and given the fact that due to the absence of external stimuli $\nabla \cdot \boldsymbol{D} = 0$, we obtain that

$$\epsilon \nabla \cdot \boldsymbol{E} = -\boldsymbol{E} \nabla \cdot \epsilon \tag{4.1.3}$$

Combining the above into the differential wave equation we see that:

$$\nabla\Big(-\frac{1}{\epsilon}\boldsymbol{E} \cdot \nabla \epsilon\Big) - \nabla^2 \boldsymbol{E} = -\mu_0 \epsilon_0 \epsilon \frac{\partial^2 \boldsymbol{E}}{\partial t^2} \Rightarrow \nabla\Big(-\frac{1}{\epsilon}\epsilon \nabla \cdot \boldsymbol{E}\Big) - \nabla^2 \boldsymbol{E} = -\frac{\epsilon}{c^2}\frac{\partial^2 \boldsymbol{E}}{\partial t^2} \tag{4.1.4}$$

and thus the wave function inside our media

$$\nabla^2 \boldsymbol{E} - \frac{\epsilon}{c^2}\frac{\partial^2 \boldsymbol{E}}{\partial t^2} = 0 \tag{4.1.5}$$

By assuming a harmonic time dependence $\boldsymbol{E}(\boldsymbol{r},t) = \boldsymbol{E}(\boldsymbol{r})e^{-i\omega t}$ of the electric field. Eq. (4.1.5) is written as:

$$\nabla^2\boldsymbol{E} + k_0^2\epsilon\boldsymbol{E} = 0, \quad k_0 = \frac{\omega}{c} \tag{4.1.6}$$

where, k_0, is the wave vector in vacuum and Eq.(4.1.6) is known as the Helmholtz equation.

4.2 Propagation Geometry

We assume for simplicity a one-dimensional problem. The EM waves propagate along the x-direction of (x, y, z) and show no spatial variation in the perpendicular, in-plane y-direction. Therefore we have that $\epsilon = \epsilon(z)$. Applied to electromagnetic surface problems, the plane $z = 0$ coincides with the interface sustaining the propagating waves, described by

$$\boldsymbol{E}(x, y, z) = \boldsymbol{E}(z)e^{i\beta x} \tag{4.2.1}$$

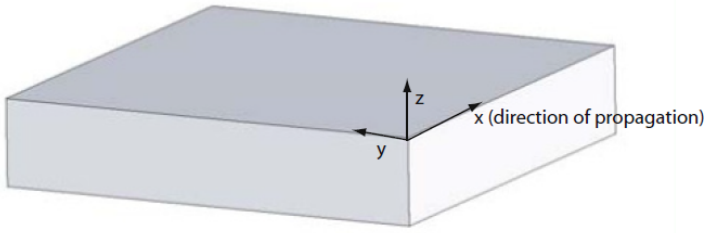

Figure 4.1: The planar propagation geometry of a waveguide in cartesian coordinates[8].

The propagation constant of traveling waves, denoted by the complex parameter $\beta = k_x$, represents the wave vector component aligned with the direction of propagation. Using it on Eq.(4.1.6) we obtain:

$$\frac{\partial^2\boldsymbol{E}(z)}{\partial z^2} + (k_0^2\epsilon - \beta^2)\boldsymbol{E} = 0 \tag{4.2.2}$$

$$\frac{\partial^2\boldsymbol{H}(z)}{\partial z^2} + (k_0^2\epsilon - \beta^2)\boldsymbol{H} = 0 \tag{4.2.3}$$

Using Maxwell's equations we have:

$$\partial_y E_z - \partial_z E_y = i\omega\mu_0 H_x \tag{4.2.4}$$
$$\partial_z E_x - \partial_x E_z = i\omega\mu_0 H_y \tag{4.2.5}$$
$$\partial_x E_y - \partial_y E_x = i\omega\mu_0 H_z \tag{4.2.6}$$
$$\partial_y H_z - \partial_z H_y = -i\omega\epsilon_0\epsilon E_x \tag{4.2.7}$$
$$\partial_z H_x - \partial_x H_z = -i\omega\epsilon_0\epsilon E_y \tag{4.2.8}$$
$$\partial_x H_y - \partial_y H_x = -i\omega\epsilon_0\epsilon E_z \tag{4.2.9}$$

For propagation along the x-direction($\partial_x \to i\beta$) and homogeneity in the y-direction ($\partial_y \to 0$) the Eqs. (4.2.4) - (4.2.9) are reshaped as follows:

$$\partial_y E_z = -i\omega\mu_0 H_x \tag{4.2.10}$$
$$\partial_z E_x - i\beta E_z = i\omega\mu_0 H_y \tag{4.2.11}$$
$$i\beta E_y = i\omega\mu_0 H_z \tag{4.2.12}$$
$$\partial_y H_z = i\omega\epsilon_0\epsilon E_x \tag{4.2.13}$$
$$\partial_z H_x - i\beta H_z = i\omega\epsilon_0\epsilon E_y \tag{4.2.14}$$
$$i\beta H_y = -i\omega\epsilon_0\epsilon E_z \tag{4.2.15}$$

We see that the system has two solutions with different polarization one for its mode (TM(p) or TE(s)). We first look at the TM mode where the non-zero components are E_x, E_z, H_y. Thus, we obtain:

$$E_x = -\frac{i}{\omega\epsilon\epsilon_0}\partial_z H_y \tag{4.2.16}$$
$$E_z = -\frac{\beta}{\omega\epsilon\epsilon_0} H_y \tag{4.2.17}$$

and the wave equation for p-modes is

$$\frac{\partial^2 H_y}{\partial z^2} + (k_0^2\epsilon - \beta^2)H_y = 0 \tag{4.2.18}$$

For the TE mode similarly we obtain

$$H_x = \frac{i}{\omega\mu_0}\partial_z E_y \tag{4.2.19}$$
$$H_z = \frac{\beta}{\omega\mu_0} E_y \tag{4.2.20}$$

and the wave equation for s-modes is

$$\frac{\partial^2 E_y}{\partial z^2} + (k_0^2\epsilon - \beta^2)E_y = 0 \tag{4.2.21}$$

4.3 Surface Plasmon Polaritons at a Single Interface

We assume that the most simple geometry for a SPP propagation is a single, flat interface between a dielectric, absorbing half space ($z > 0$) with positive dielectric constant $\epsilon_2 = \epsilon_r + i\epsilon_i$,where ϵ_r is the $\Re(\epsilon_2)$, ϵ_i is the $\Im(\epsilon_2)$ or the "gain" coefficient for our dielectric material and an adjacent conducting half space ($z < 0$) described via a dielectric function:

$$\epsilon_1 = \epsilon(\omega) = 1 - \frac{\omega_p^2}{\omega^2 + i\gamma\omega} \tag{4.3.1}$$

where ω_p is the plasmon's frequency and γ is the loss coefficient for our metal.

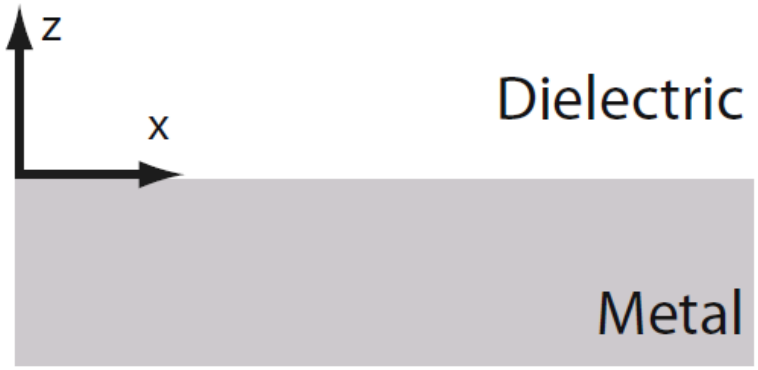

Figure 4.2: Depicting the planar propagation geometry of a single interface of dielectric/metal for a surface plasmon polariton.

We first examine the TM modes. From our solutions (4.2.16) and (4.2.17) we obtain in both half spaces, for $z > 0$:

$$E_x(z) = -iA_1\frac{k_2}{\omega\epsilon_2\epsilon_0}e^{i\beta x}e^{-k_2 z} \tag{4.3.2}$$

$$E_z(z) = A_2\frac{\beta}{\omega\epsilon_2\epsilon_0}e^{i\beta x}e^{-k_2 z} \tag{4.3.3}$$

$$H_y(z) = A_2 e^{i\beta x}e^{-k_2 z} \tag{4.3.4}$$

and for $z < 0$

$$E_x(z) = -iA_1 \frac{k_1}{\omega \epsilon_1 \epsilon_0} e^{i\beta x} e^{k_1 z} \tag{4.3.5}$$

$$E_z(z) = -A_1 \frac{\beta}{\omega \epsilon_1 \epsilon_0} e^{i\beta x} e^{k_1 z} \tag{4.3.6}$$

$$H_y(z) = A_1 e^{i\beta x} e^{k_1 z} \tag{4.3.7}$$

where $k_j = k_{z,j}$, $j = 1, 2$ is the component of the wave vector perpendicular to the interface in the two media.

We now depict below the electric field distribution of the rectangular geometry of the SPP

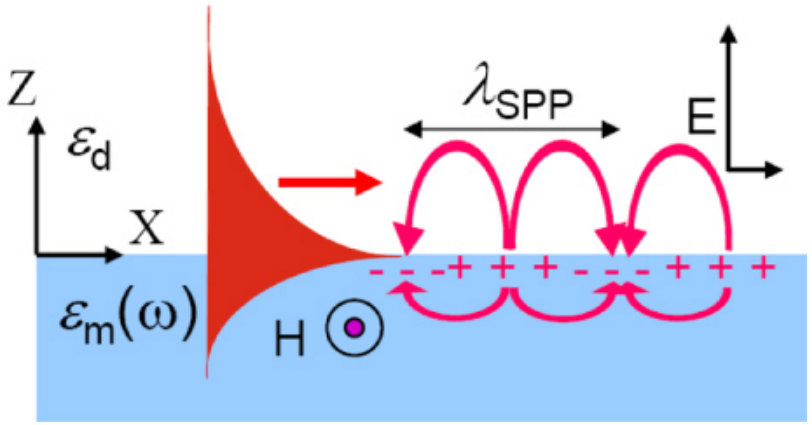

Figure 4.3: The electric field distribution of a SPP in a plane geometry.

The relation between the k_j and ϵ_j for $j = 1, 2$ is:

$$\frac{k_2}{k_1} = -\frac{\epsilon_2}{\epsilon_1} \tag{4.3.8}$$

We also know that the wavevectors k_j and β, the propagation constant are releated with the following equations:

$$k_j^2 = \beta^2 - k_0^2 \epsilon_j \qquad j = 1, 2 \tag{4.3.9}$$

$$k_0 = \frac{\omega}{c} \tag{4.3.10}$$

Thus we obtain the relation between β, ϵ_j and k_0:

$$\beta = k_0 \sqrt{\frac{\epsilon_1 \epsilon_2}{\epsilon_1 + \epsilon_2}} \tag{4.3.11}$$

To continue with, we now examine the TE modes. The equations that emerge, for $z > 0$, are

$$H_x(z) = -iA_2 \frac{k_2}{\omega \mu_0} e^{i\beta x} e^{-k_2 z} \tag{4.3.12}$$

$$H_z(z) = A_2 \frac{\beta}{\omega \mu_0} e^{i\beta x} e^{-k_2 z} \tag{4.3.13}$$

$$E_y(z) = A_2 e^{i\beta x} e^{-k_2 z} \tag{4.3.14}$$

and for $z < 0$

$$H_x(z) = iA_1 \frac{k_1}{\omega \mu_0} e^{i\beta x} e^{k_1 z} \tag{4.3.15}$$

$$H_z(z) = A_1 \frac{\beta}{\omega \mu_0} e^{i\beta x} e^{k_1 z} \tag{4.3.16}$$

$$E_y(z) = A_1 e^{i\beta x} e^{k_1 z} \tag{4.3.17}$$

Impling the continuity of E_y and H_x we see that $A_1(k_1 + k_2) = 0$. This implies $A_1 = 0 = A_2(\Re[k_1], \Re[k_2] > 0)$. Therefore we see that there is no existance of TE polarization, but only for TM.

Replacing k_0 with ω/c we solve the above equation and we have our final dispersion relation $\omega - \beta$:

$$\beta^2 - \frac{\omega^2}{c^2} \frac{(1 - \frac{\omega_p^2}{\omega^2 + i\gamma\omega})(\epsilon_r + i\epsilon_i)}{(1 - \frac{\omega_p^2}{\omega^2 + i\gamma\omega} + \epsilon_r + i\epsilon_i)} = 0 \tag{4.3.18}$$

which ends up giving us the following initial dispersion relation between ω and β, respectively. We have that:

$$\frac{c^2\beta^2(\omega(i\gamma + \omega)(i\varepsilon_i + \varepsilon_r + 1) - \omega_p^2) + \omega^2(i\varepsilon_i + \varepsilon_r)(-i\gamma\omega - \omega^2 + \omega_p^2)}{c^2(\omega(i\gamma + \omega)(i\varepsilon_i + \varepsilon_r + 1) - \omega_p^2)} = 0 \tag{4.3.19}$$

First we have to check for which values of ω, the denominator is 0. We see that

$$c^2(\omega(i\gamma + \omega)(i\varepsilon_i + \varepsilon_r + 1) - \omega_p^2) = 0 \tag{4.3.20}$$

And therefore we obtain the two solutions:

$$\omega_{\pm} = \frac{-i\gamma \pm \sqrt{-\gamma^2 + \frac{4\omega_p^2}{1+\epsilon_r+i\epsilon_i}}}{2} \tag{4.3.21}$$

We see that those solutions do not match with the solutions of the dispersion relation that we have. Therefore we can procceed with the nominator being 0. Thus we have:

$$c^2\beta^2(\omega(i\gamma+\omega)(i\varepsilon_i+\varepsilon_r+1)-\omega_p^2)+\omega^2(i\varepsilon_i+\varepsilon_r)(-i\gamma\omega-\omega^2+\omega_p^2)=0 \tag{4.3.22}$$

The above equation results in a polynomial with degree equal to $d = 4$

$$\epsilon_2\omega^4 + i\gamma\epsilon_2\omega^3 - (c^2\beta^2(1+\epsilon_2)+\epsilon_2\omega_p^2)\omega^2 - c^2\beta^2 i\gamma(1+\epsilon_2)\omega + c^2\beta^2\omega_p^2 = 0 \tag{4.3.23}$$

For a lossless metal, $\gamma = 0$, we obtain the following dispersion curve:

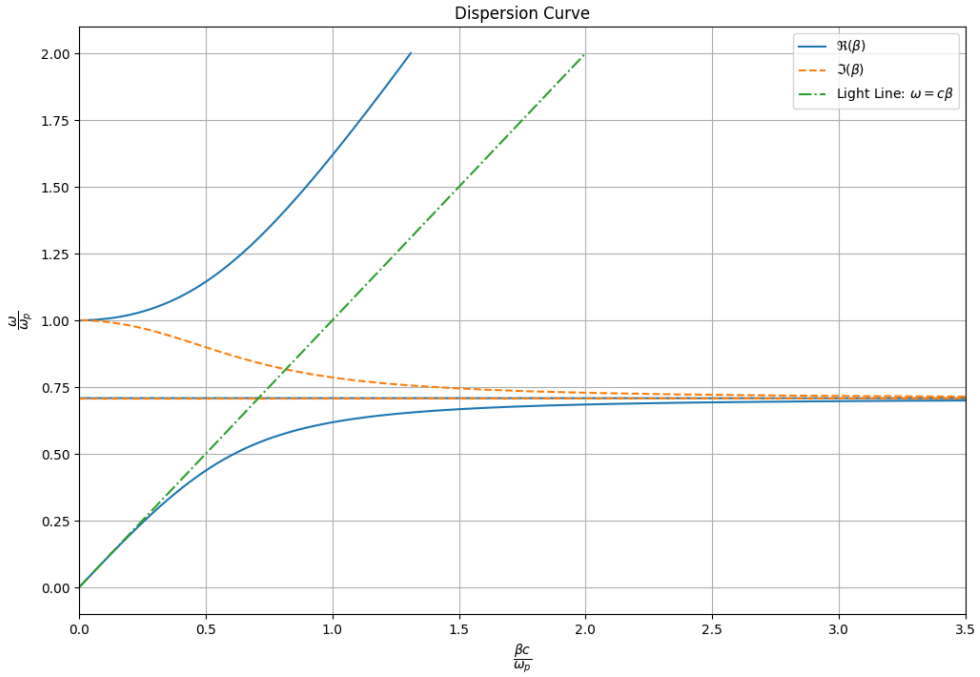

Figure 4.4: The dispersion relation $\omega - \beta$ of a SPP in a single interface with negligible damping ($\gamma = 0$). The blue-orange-dashed line depicts the frequency of the surface plasmon ω_{sp}. Both ω and β are normalized[6].

We must investigate SPPs' attributes. The SPP excitations correspond to the portion of the dispersion curve that is to the right of the respective light line of air, according to the preceding figure for minimal damping from the Drude metal and air as the dielectric. We can see that when $\omega > \omega_p$, radiation into the metal occurs.The domain of the bound and surface plasmon modes have a frequency gap region with pure $\Im(\beta)$ that does not permit SPP propagation. The SPP propagation constant is near to k_0 at the light line for tiny wave vectors β associated with lower frequencies, and the waves spread over a wide range of wavelengths into the dielectric space.

In the opposite limit of large wave vectors, the frequency of the SPPs approaches the surface plasmon frequency

$$\omega_{sp} = \frac{\omega_p}{\sqrt{1+\epsilon_2}} \tag{4.3.24}$$

The plasmon's dispersion relation can be demonstrated by including the free-electron dielectric function. The wave vector β increases to infinity as the frequency approaches $\omega_s p$ and the group velocity $v_g \to 0$ in the case of negligible damping of the conduction electron oscillation, which

implies that $\Im(\epsilon_1(\omega)) = 0$. The mode now has an electrostatic quality, and is called a surface plasmon[13][14].

Solving the Laplace equation for the single interface geometry, where ϕ is the electric potential, yields the same results as the prior method[11][4]. The equation yields a solution that is exponentially declining in the z direction and wavelike in the x direction.

$$\phi(z) = A_2 e^{i\beta x} e^{-k_2 z} \tag{4.3.25}$$

for $z > 0$ and

$$\phi(z) = A_1 e^{i\beta x} e^{k_1 z} \tag{4.3.26}$$

for $z < 0$. $\nabla^2\phi = 0$ requires that $k_1 = k_2 = \beta$: the exponential decay lengths $|\hat{z}| = 1/k_z$ into the dielectric and into the metal are equal. Continuity of ϕ and $\epsilon\partial\phi/\partial z$ ensure continuity of the tangential field components and the normal components of the dielectric displacement and require that $A_1 = A_2$ and additionally

$$\epsilon_1(\omega) + \epsilon_2 = 0 \tag{4.3.27}$$

This requirement is satisfied at $\omega_s p$ for a metal described by a dielectric function such as Eq. (4.2.2) Consequently, we can see that the surface plasmon is really in the limiting form of an SPP as $\beta \to \infty$ by comparing the dispersion relation with the dielectric function equation.

These results imply for a Drude metal with negligible damping ($\Im(\epsilon_1) = 0$). Real metals include the damping factor γ as we mentioned in the beginning of the paragraph. Therefore, $\epsilon_1(\omega)$ is complex, and with it also the SPP propagation constant β. The travelling SPPs are damped with an energy attenuation length(also called propagation length) $L = (2\Im(\beta))^{-1}$. Some typical numbers for the propagation length stand between 10 and 100 μm in the visible regime, depending upon the metal/dielectric configuration.

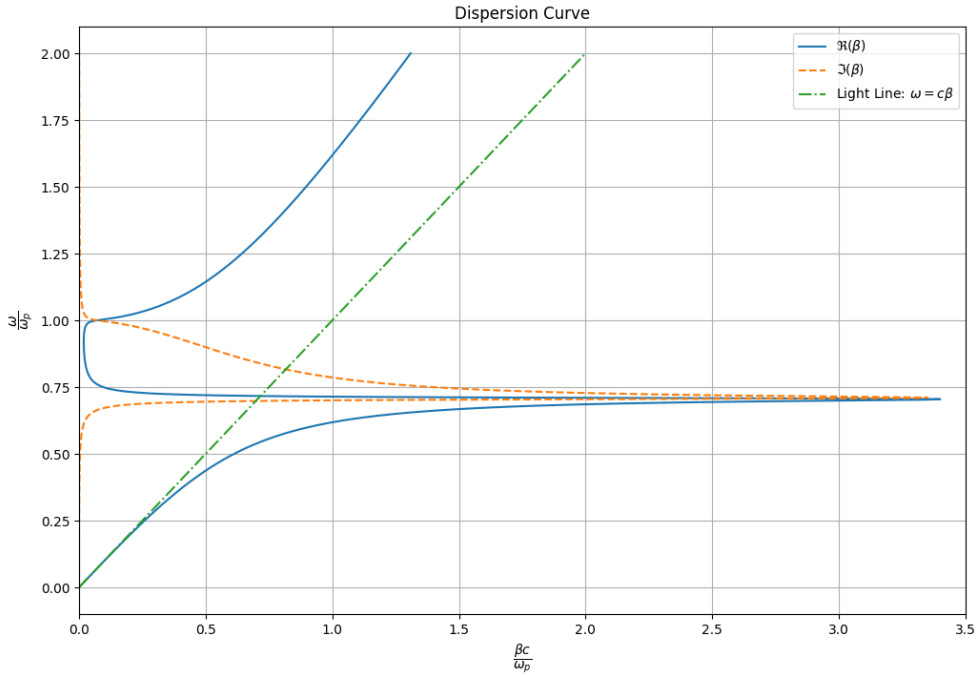

Figure 4.5: The dispersion relation $\omega - \beta$ of a SPP in a single interface with damping ($\gamma = 0.01$). Now ω, γ and β are normalized[6].

The above figure shows the dispersion relation of SPPs propagating at a metal/air interface, with the dielectric function $\epsilon_1(\omega)$ of the metal having losses. Compared with the dispersion relation of completely undamped SPPs as we depicted before, it can be seen that the bound SPPs approach now a maximum, finite wave vector at the surface plasmon frequency ω_{sp} of the system above. This limitation puts a lower bound both on the wavelength $\lambda_{sp} = 2\pi/\Re(\beta)$ of the surface plasmon and also on the amount of mode confinement perpendicular to the interface, since the SPP fields in the dielectric fall as $e^{-|k_z||z|}$ with $k_z = \sqrt{\beta^2 - \epsilon_2\left(\frac{\omega}{c}\right)^2}$. In contrast to the situation of an ideal metal, the quasibound, leaky portion of the dispersion relation between $\omega_s p$ and ω_p is now permitted.

4.4 Active Dielectric - PT Gain

In this part, we examine how the Drude metal losses in SPP propagation can be balanced by introducing gain into the dielectric[10][9]. Gain materials have a complex permittivity function with the formula $\epsilon_d = \epsilon_d' + i\epsilon_d''$, where $\epsilon_d', \epsilon_d'' > 0$, where ϵ_d'' is a small value in comparison to ϵ_d' and accounts for gain[16]. Additionally, active dielectrics have been used to investigate PT symmetry in optical systems defined by the requirement that $n(-x) = n^*(x)$, where n, n^*, and x denote

the spatial coordinate along the interface and correspondingly the refractive index and its complex conjugate. Gain dielectrics and loss metals can be used to create meta-materials with PT symmetric effective refractive indices. PT symmetric media are intriguing because they permit EM control.

The dispersion relation $\omega - \beta$ can be also written as $\beta = k_0 n_{sp}$, where n_{sp} is the plasmon effective refractive index given by

$$n_{sp} = \sqrt{\frac{\epsilon_d \epsilon_m}{\epsilon_d + \epsilon_m}} \tag{4.4.1}$$

The effective index n_{sp} must become real for us to get the benefit ϵ_d''. The function $n_s p$ is represented in the ordinary complex form as by substituting the complex function characterizing the metal and dielectric into the dispersion relation. Hence, we have that

$$n_{sp} = \sqrt{\frac{\sqrt{x^2+y^2}+x}{2}} + isgn(y)\sqrt{\frac{\sqrt{x^2+y^2}-x}{2}} \tag{4.4.2}$$

where $sgn(y)$ is the discontinuous signum function and

$$x = \frac{\epsilon_d' |\epsilon_m|^2 - \epsilon_m' |\epsilon_d|^2}{|\epsilon_d + \epsilon_m|^2} \tag{4.4.3}$$

$$y = \frac{\epsilon_d'' |\epsilon_m|^2 - \epsilon_m'' |\epsilon_d|^2}{|\epsilon_d + \epsilon_m|^2} \tag{4.4.4}$$

with the $|\epsilon_j|$ denoting the norm of the complex number ϵ_j, where $j = d, m$. The poles of x, y correspond to the nonretarded surface plasmon limit

$$\epsilon_d + \epsilon_m = 0 \tag{4.4.5}$$

When the requirements $y = 0$ and $x > 0$ are met at the same time, lossless propagation of the plasmon effective index n_{sp} is warranted, as shown by the observation that $(\Im(n_{sp}) = \Im((b)) = 0)$. The imaginary portion of n_{sp} vanishes for $y = 0$ and $x0$ due to the signum function, but its real part becomes imaginary, i.e., $n_{sp} = i\sqrt{|x|}$, which does not correspond to propagation waves. We find two exact solutions to the equation $y = 0$ by solving it with respect to gain ϵ_d'' and avoiding the nonretarded limit, which is $\epsilon_d \neq \epsilon_m$. From the above we solve for ϵ_d'' and we get that

$$\epsilon_{d,\pm}'' = \frac{|\epsilon_m|^2}{2\epsilon_m''}\left(1 \pm \sqrt{1 - \left(\frac{2\epsilon_d' \epsilon_m''}{|\epsilon_m|^2}\right)^2}\right) \tag{4.4.6}$$

Due to the fact that ϵ_d is real, we read from the above equation that

$$|\epsilon_m|^2 \geq 2\epsilon'_d\epsilon''_m \tag{4.4.7}$$

With the help of the aforementioned inequality, we can deduce that $\epsilon''_d > \epsilon'_d$ is not the solution. Since the ϵ''_d is defined to be smaller than the ϵ'_d, this is a contradiction. So, $\epsilon''_{d,+}$ does not correlate to a gain that is meaningful in terms of physical reality.

Solving, on the other hand $y = 0$ for $x > 0$, with respect to the dielectric gain ϵ''_d, we determine a critical value ϵ_c distinguishing the regimes of lossless and prohibited SPP propagation, namely

$$\epsilon_c = \epsilon'_d\sqrt{\frac{|\epsilon_m|^2}{\epsilon'_m\epsilon'_d} - 1} \tag{4.4.8}$$

Consequently, ϵ_c establishes a maximum gain value. The appearance of critical gain can be explained by the following equation: the gain $\epsilon_{d,-}$ becomes equal to ϵ_c when $\epsilon_d + \epsilon_m = 0$, where the last item is the nonretarded limit when $\beta \to \infty$. In particular, the Drude dielectric function $\epsilon(\omega)$, $\epsilon''_{d,-} = \epsilon_c$ at $\omega = \omega_{sp}$, or a maximum frequency, indicates the presence of the surface plasmon.

The fact that the refractive index n meets the requirement that $n(y = 0) = n^*(y = 0)$ since its imaginary portion vanishes as a result of the signum function is an intriguing aspect of the lossless SPP propagation scenario, or for $\epsilon''_{d,-} < \epsilon_c$. With n being spatially independent, this may thus be viewed as the $\mathcal{PT}$ symmetry phase requirement. The structure is not mathematically PT symmetric in the strict sense, but time-reversal and geometrical symmetry are permitted by the real value of the supported propagation constant along the interface. Then, the dielectric gain expression $\epsilon''_{d,-}$, represented as $\epsilon''_{d,-} \equiv \epsilon_{\mathcal{PT}}$, can be attributed to the $\mathcal{PT}$ symmetry property provided by the lossless SPP propagation. The following will preserve the denomination. The $\mathcal{PT}$ condition is not met in the case of $\epsilon''_{d,-} > \epsilon_c$, however, because the refractive index is imaginary, the crucial gain ϵ_c may then be viewed as the plasmonic system analysis' $\mathcal{PT}$-symmetry breaking point.

Below we present the results

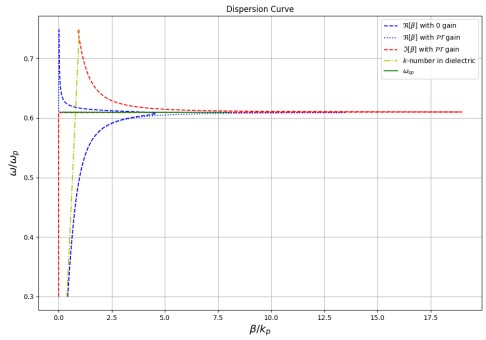

Figure 4.6: The lossless propagation of a $\mathcal{PT}$ plasmon, where gain is added to counterbalance the losses

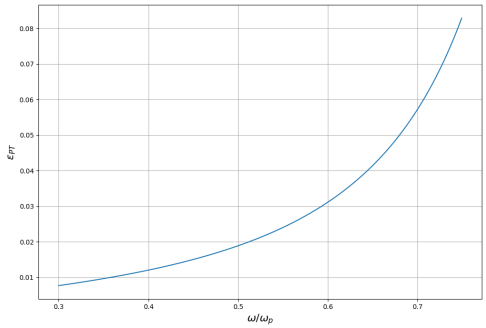

Figure 4.7: The gain-frequency diagram in the range of $[0.3\omega_p, 0.75\omega_p]$ with step $0.001\omega_p$.

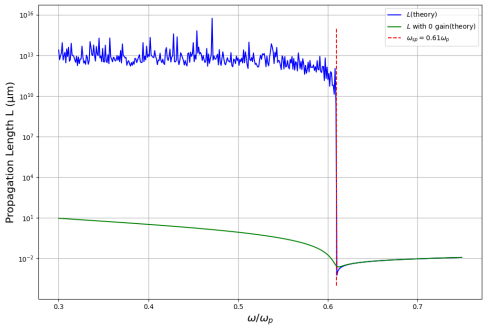

Figure 4.8: Plotting the propagation Length L with respect of the normalized frequency within the same range as Fig. 5.7. We see that the amplified SPP now has significantly larger L than the one without gain/loss.

4.5 Surface Plasmon Polaritons at a Bi-Layer System

We study now, SPPs in multilayers consisting of alternating conducting and dielectric thin films. In a system like that, each single interface can sustain bound SPPs. Interactions between SPPs result in linked modes when the distance between consecutive interfaces is equal to or less than the interface mode's decay length $\hat{z}$. We will concentrate on two distinct three-layer systems in order to clarify the overall characteristics of coupled SPPs. First, an insulator/metal/insulator (IMI) heterostructure composed of a thin metallic layer (I) sandwiched between two (infinitely) thick dielectric claddings (II, III), and second, a metal/insulator/metal (MIM) heterostructure composed of a thin dielectric core layer (I) sandwiched between two metallic claddings (II, III)[2].

We depict the geometry below

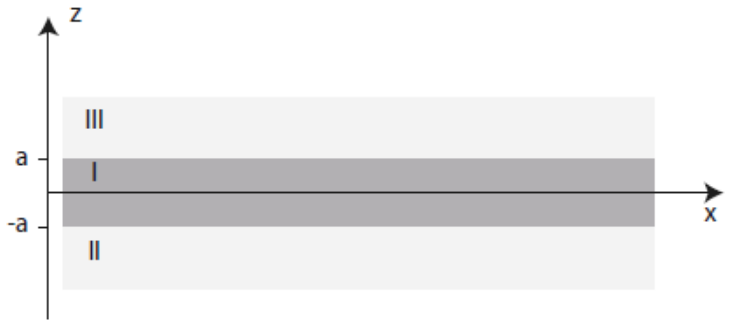

Figure 4.9: The propagation geometry of the bi-layer interface[8].

Since we are only interested in the lowest-order bound modes, we start with a general description of the TM modes that are non-oscillatory in the $z-$direction normal to the interfaces.

For $z > a$, the field components are

$$H_y = Ae^{i\beta x}e^{-k_3 z} \tag{4.5.1}$$

$$E_x = iA\frac{1}{\omega\epsilon_0\epsilon_3}k_3 e^{i\beta x}e^{-k_3 z} \tag{4.5.2}$$

$$E_z = -A\frac{\beta}{\omega\epsilon_0\epsilon_3}e^{i\beta x}e^{-k_3 z} \tag{4.5.3}$$

where for $z < -a$ we have that

$$H_y = Be^{i\beta x}e^{k_2 z} \tag{4.5.4}$$

$$E_x = -iB\frac{1}{\omega\epsilon_0\epsilon_2}k_2 e^{i\beta x}e^{k_2 z} \tag{4.5.5}$$

$$E_z = -B\frac{\beta}{\omega\epsilon_0\epsilon_2}e^{i\beta x}e^{k_2 z} \tag{4.5.6}$$

Hence, the fields must decay exponentially in the claddings (II) and (III).

In the core region $-a < z < a$, the modes localized at the bottom and top interface couple, yielding to

$$H_y = Ce^{i\beta x}e^{k_1 z} + De^{i\beta x}e^{-k_1 z} \tag{4.5.7}$$

$$E_x = -iC\frac{1}{\omega\epsilon_0\epsilon_1}k_1 e^{i\beta x}e^{k_1 z} + iD\frac{1}{\omega\epsilon_0\epsilon_1}k_1 e^{i\beta x}e^{-k_1 z} \tag{4.5.8}$$

$$E_z = C\frac{\beta}{\omega\epsilon_0\epsilon_1}e^{i\beta x}e^{k_1 z} + D\frac{\beta}{\omega\epsilon_0\epsilon_1}e^{i\beta x}e^{-k_1 z} \tag{4.5.9}$$

The requirement of continuity of H_y and E_x for $z = a$ leads to the following relations

$$Ae^{-k_3 a} = Ce^{k_1 a} + De^{-k_1 a} \tag{4.5.10}$$

$$\frac{A}{\epsilon_3}k_3 e^{-k_3 a} = -\frac{C}{\epsilon_1}k_1 e^{k_1 a} + \frac{D}{\epsilon_1}k_1 e^{-k_1 a} \tag{4.5.11}$$

and for $z = -a$ we have that

$$Be^{-k_2 a} = Ce^{-k_1 a} + De^{k_1 a} \tag{4.5.12}$$

$$-\frac{B}{\epsilon_2}k_2 e^{-k_2 a} = -\frac{C}{\epsilon_1}k_1 e^{-k_1 a} + \frac{D}{\epsilon_1}k_1 e^{k_1 a} \tag{4.5.13}$$

Thus we obtain a linear system of four coupled equations.

Solving the above system results in a implicit expression for the dispersion relation linking β and ω via

$$e^{-4k_1 a} = \frac{k_1/\epsilon_1 + k_2/\epsilon_2}{k_1/\epsilon_1 - k_2/\epsilon_2}\frac{k_1/\epsilon_1 + k_3/\epsilon_3}{k_1/\epsilon_1 - k_3/\epsilon_3} \tag{4.5.14}$$

We can see that if we have an infinite thickness of the metal ($a \to \infty$) the two coupled SPPs become uncoupled at the respective interfaces.

We select the two dielectric claddings to be the same. Thus we obtain $k_2 = k_3$. Hence $\epsilon_2 = \epsilon_3$. In this case, the dispersion relation can be split into a pair of equations, hence

$$\tanh k_1 a = -\frac{k_2\epsilon_1}{k_1\epsilon_2} \tag{4.5.15}$$

$$\coth k_1 a = -\frac{k_2\epsilon_1}{k_1\epsilon_2} \tag{4.5.16}$$

We can show that the first equation describes modes of odd vector parity($E_x(z)$ is odd, $H_y(z)$ and $E_z(z)$ are even functions), while the second equation describes modes of even vector parity($E_x(z)$ is even, $H_y(z)$ and $E_z(z)$ are odd functions). The above dispersion relations can now be applied to both IMI and MIM structures in order to investigate the properties of the coupled SPP modes in these two systems.

Below we present the odd and even modes of the bi-layer system

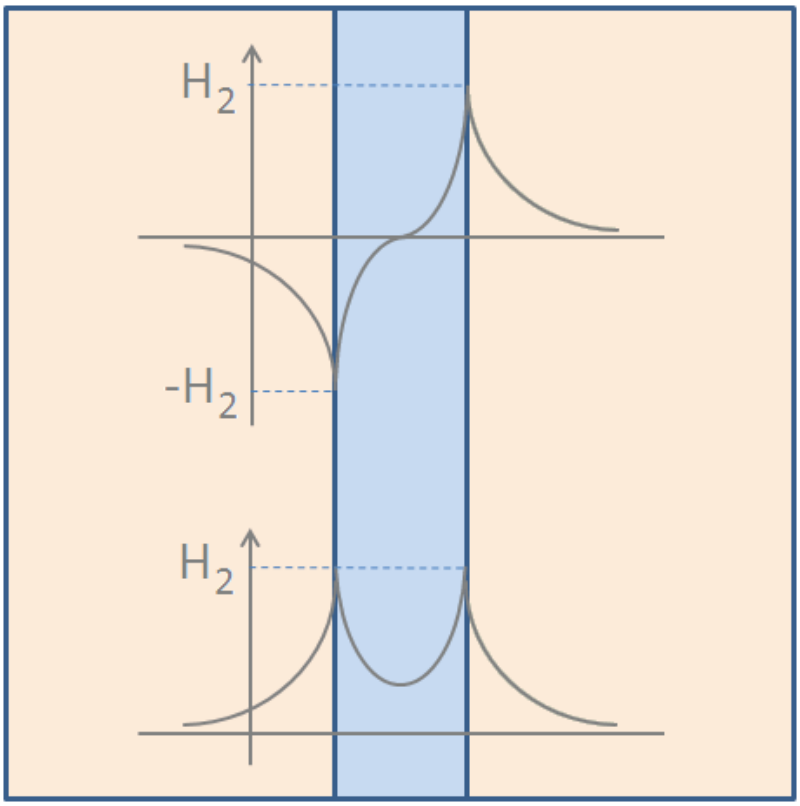

Figure 4.10: The hybridization of the two modes in the bi-layer geometry. The upper mode represent the field magnitude of the the antisymmetric (odd one), where the lower mode represent the field magnitude of the symmetric (even one).

We first start with the IMI geometry where we depict a thin metallic layer of thickness equals to $2a$. Thus the dielectric function $\epsilon_1 = \epsilon_1(\omega)$ is for the metal and ϵ_2 is the dielectric constant, positive and real, of the insulating sub- and superstrates. We now draw the dispersion relation $\omega - \beta$ of this system. Hence, we have

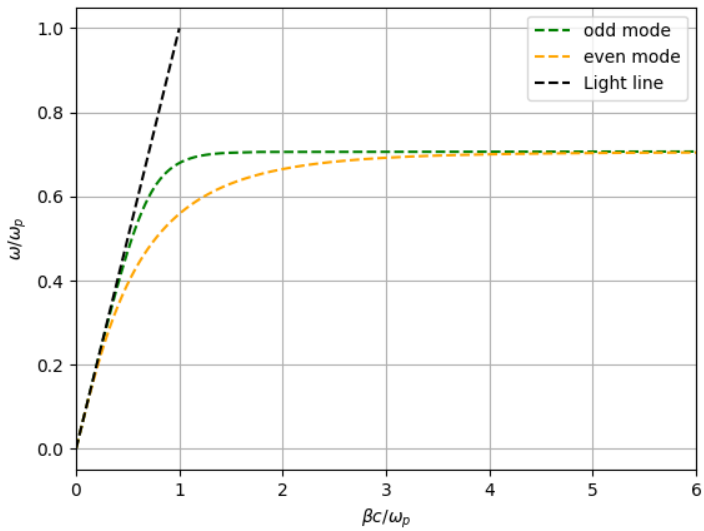

Figure 4.11: The dispersion relation of an IMI geometry where the metal is represented as a Drude model with negligible damping ($\gamma = 0$). Both ω and β are normalised[8][3][6].

Here for simplicity we have chosen the dielectric function of silver being approximated via a Drude model with negligible damping, hence $\Im(\beta) = 0$. For large wave vectors β we have that the modes $\omega_{\pm}$(which are only achievable if $\Im(\epsilon(\omega)) = 0$) have a limit and that is

$$\omega_{\pm} = \frac{\omega_p}{\sqrt{1+\epsilon_2}} \sqrt{1 \pm \frac{2\epsilon_2 e^{-2\beta a}}{1+\epsilon_2}} \tag{4.5.17}$$

The $(+)$ symbolizes the odd modes and the $(-)$ the even modes.

When we add losses to the metal the dispersion relation diagram transforms as follows

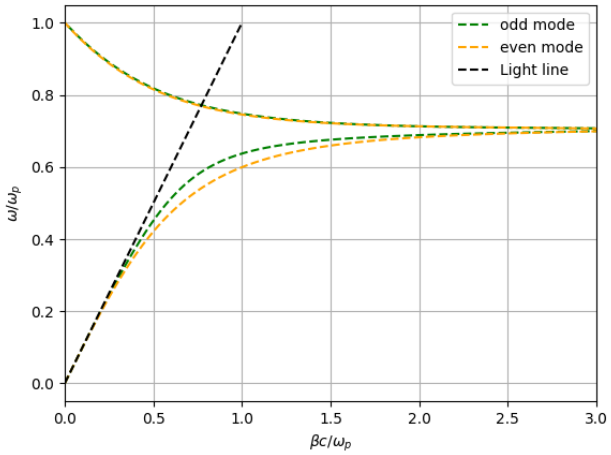

Figure 4.12: The dispersion relation of an IMI geometry where the metal is represented as a Drude model with damping ($\gamma = 0.01$). Both ω and β are normalised[6].

We see that the two modes are combined as one mode after the surface plasmon frequency and lead to a finite limit of the wave vector.

We now move on to the MIM geometry, where we depict a thin insulating core sandwiched between two metals. We set now $\epsilon_2 = \epsilon_2(\omega)$. We depict the dispersion relation below

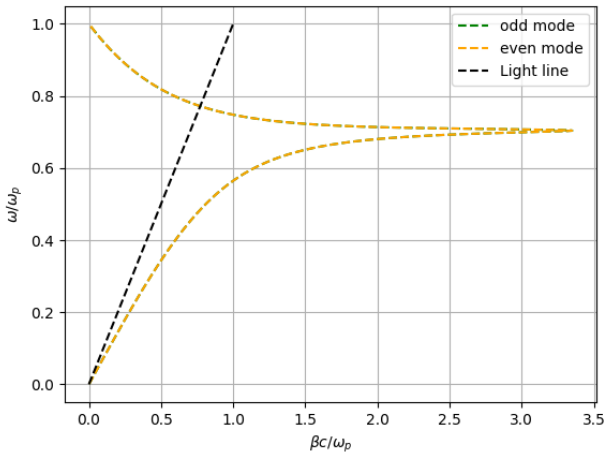

Figure 4.13: The dispersion relation of a MIM geometry where the metal is represented as a Drude model with damping ($\gamma = 0.01$). Both ω and β are normalised[6].

We see that the now we have only one mode (the two modes are matched). Now that the dielectric function has both real and imaginary part we see the losses in the dispersion relation as a finite limit of the wave vector. Hence, β does not go to infinity as the surface plasmon frequency ω_{sp} is approached. It kindly reminds of the single layer SPP propagation[5].

Chapter 5

Simulations

In this section we performed some simulations using the COMSOL Multiphysics® software in order to verify our results. We construct a $2D$ space for the purpose to study in the frequency domain the EM waves in the rectangular geometry for TM polarization electric field. Precisely, we want to calculate the SPPs propagation length L with respect to the normalised frequency ω/ω_p. We perform this simulation for the single interface geometry with an active dielectric and a Drude metal. We want to study the behavior from the lossless to prohibited propagation for the SPP.

We will start by constructing the geometry in COMSOL. We create a rectangular geometry with legnth $L = 2\mu m$ and height $H = 3\mu m$. We continue by splitting the geometry in to two layers. The Drude's metal layer which has height equal to $H/4$ of the whole geometry and the rest belongs to the dielectric. Furthermore we insert materials for each layer. For the metal we choose silver and for the dielectric, air.

We continue now the study of the EM wave and the frequency domain. Because we inserted materials, from the library of COMSOL we can take the data of each materials refractive index and insert it to the dispersion equation. Now we initiate from the left side of the geometry an active port from which the EM wave will propagate. In order for this to work properly we have to put another port at the right side of the geometry, in order to work as a boundary condition and terminate the propagation. This port must be inactive.

Continuing with the mesh of the geometry, we choose a custom mesh from the general physics category and fix the parameters for each element size to be $max = 125nm$ and $min = 0.6nm$, in order to have a very detailed grid.

Going to the final step, that is to select the frequency domain to be set from the wavelength of the metal. That is the wave length domain from $340nm - 600nm$ with a step of $10nm$ for each iteration. Below we present the results.

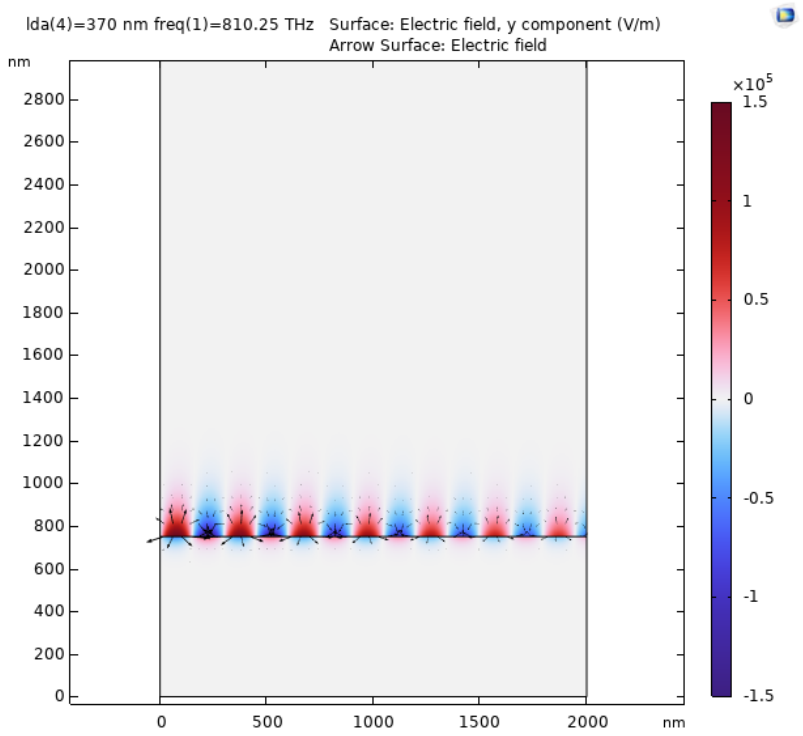

Figure 5.1: Simulation of a SPP electric field, propagating in a single interface of silver/air geometry with damping and no gain.

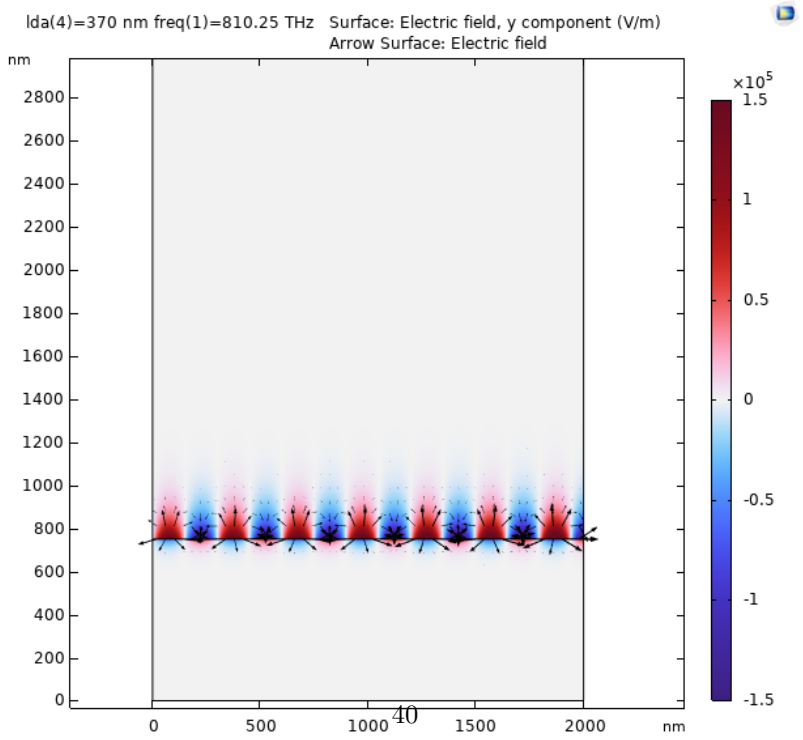

Figure 5.2: Simulation of a SPP electric field, propagating in a single interface of silver/air geometry with damping and with $\mathcal{PT}$ gain.

Below we depict the simulated dispersion relation from COMSOL software.

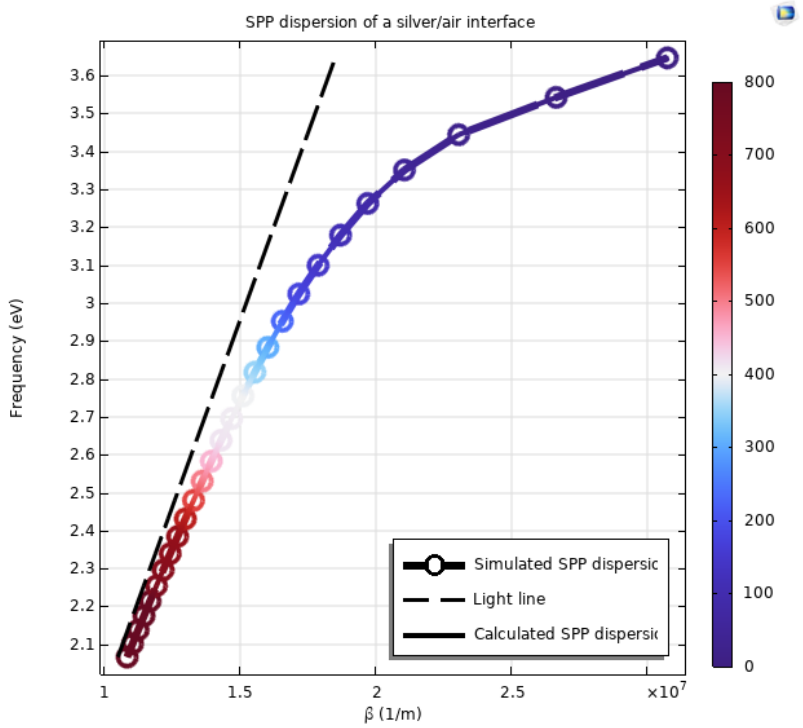

Figure 5.3: Simulating the dispersion relation of a SPP in a sivler/air interface. On the $x-$axis we have the propagation constant β in m^{-1} and on $y-$axis we have the frequency in eV.

We now continue to the multi-layer geometry where we depict the modes (symmetric and anti-symmetric) of the electric field.

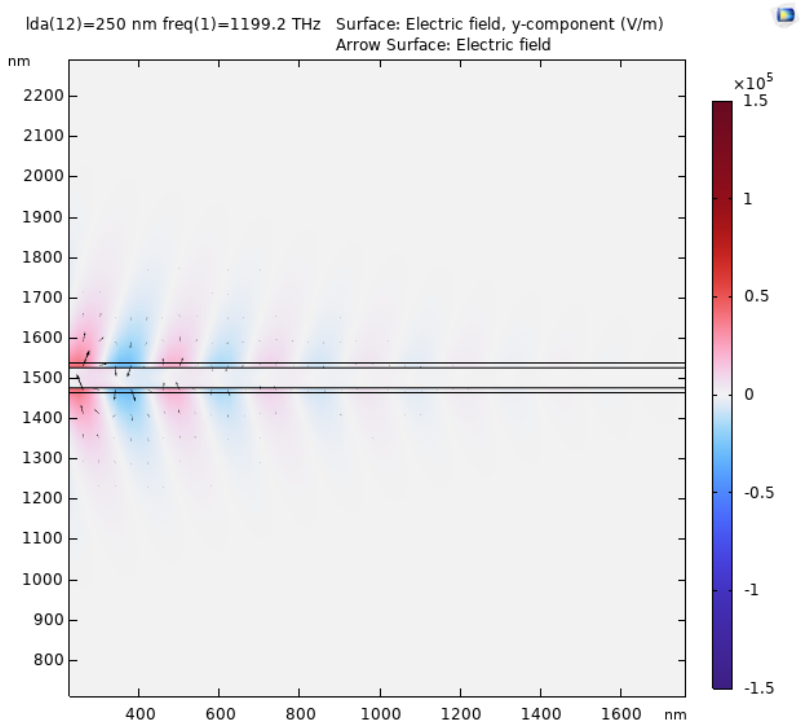

Figure 5.4: Simulation of a SPP symmetric electric field mode(even), propagating in a bi-layer interface of air/silver/air geometry with damping and no gain.

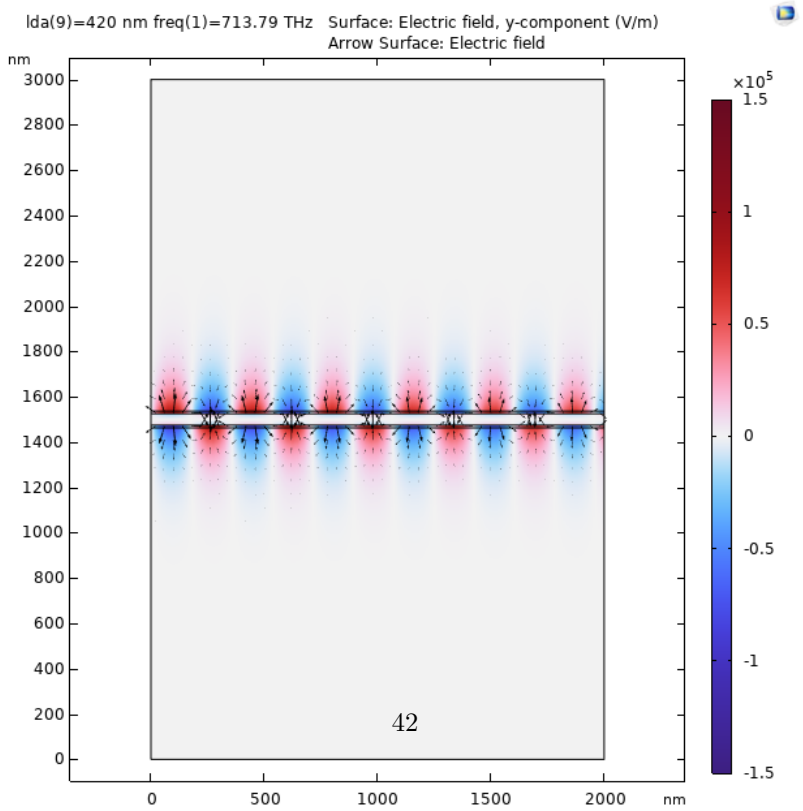

Figure 5.5: Simulation of a SPP anti-symmetric electric field mode(odd), propagating in a bi-layer interface of air/silver/air geometry with damping and no gain.

We now continue with a simulation of a $2D$ material, graphene. The advantage of graphene is that it can radiate in the IR regime where, noble metals in general have a plasma frequency near UV. We perform a simulation where graphene is sandwiched in air/SiO_2 claddings. We create a very thin graphene layer and we fix the dielectric function of graphene from its conductivity current σ.

We depict below the electric field and the dispersion relation of that IMI geometry.

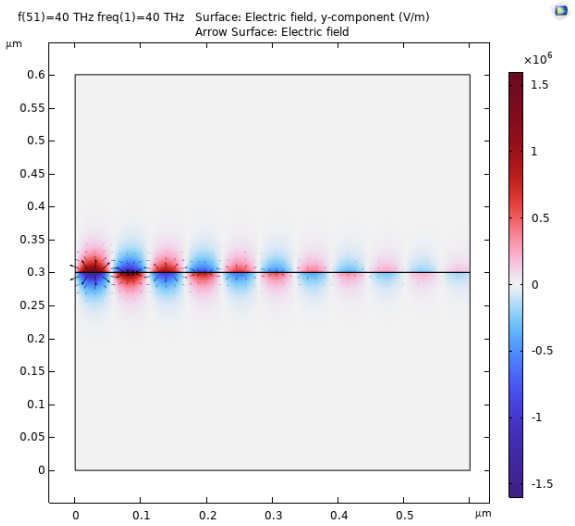

Figure 5.6: Simulation of a SPP electric field, propagating in graphene.

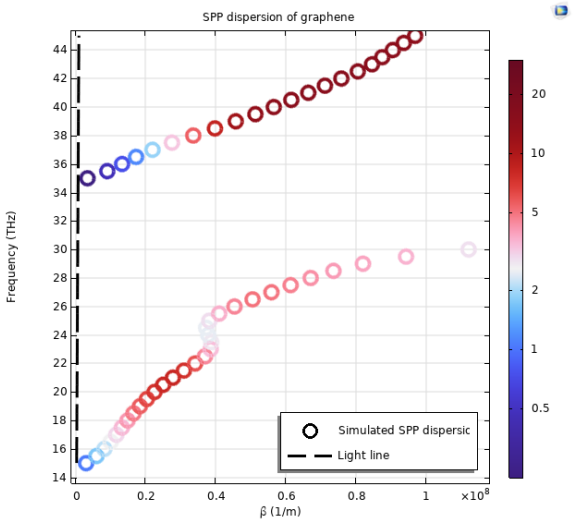

Figure 5.7: Simulation of the dispersion relation of graphene SPP.

Chapter 6

Conclusion

Summarizing we have studied SPPs at a single interface and multi interface geometry. We saw that for the single interface geometry there is an explicit function for adding gain to the dielectric material in order to counterbalance the losses. We found also that there is a critical gain and beyond that we don't obtain a SPP propagation. For the multilayer system in order to find the gain we have to solve it numerically and see when the $\Im(\beta) = 0$. The gain factor for the dielectric has similar properties for the system as the $\mathcal{PT}$ symmetry. We also performed COMSOL simulations to verify our theoretical results. There is work to be done regarding the multilayer system with gain saturation in order to find an analytical expression for the gain factor $\epsilon_{\mathcal{PT}}$.

Appendix

Python Code for Plasmonics

```
#!/usr/bin/env python
# coding: utf-8

# # Import Libraries

# In[1]:


import numpy as np
from scipy.optimize import fsolve
import matplotlib.pyplot as plt
import sympy as sp


# # Bulk Plasmon

# In[ ]:


with np.errstate(divide='ignore'):
    eq_bulk = sp.simplify(sp.sqrt(w**2 -1))
func_bulk = sp.lambdify(w,eq_bulk)
omega = np.linspace(0,2,1000)
beta_bulk = func_bulk(omega)
plt.figure(figsize = (12,8))
plt.plot(beta_bulk,omega,'-')
plt.plot(omega,omega,'-.')
plt.xlabel(r'$\dfrac{ c }{ _p }$')
plt.ylabel(r'$\dfrac{  }{ _p }$')
plt.title("Dispersion Curve")
plt.legend([r"Bulk Plasmon",r"Light Line"])
plt.grid()


# # Single-Layer Interface

# In[ ]:


w,g,k,a,wp, c, re, kp = sp.symbols("\omega \gamma \kappa a \omega_p c e_d k_p", real
    = True)
```

```
b = sp.symbols("b")


# # Negligible Damping

# In[ ]:


with np.errstate(divide='ignore'):
    eq = sp.simplify(w *sp.sqrt((1+0.j)*(1- 1/(w**2+1j*w*g))/(1+0.j+(1-1/(w**2+1j*w*
    g)))))
    eq = eq.evalf(subs = {g:1e-200})
func = sp.lambdify(w,eq)
omega = np.linspace(0,2,1000)
beta = func(omega)
plt.figure(figsize = (12,8))
plt.plot(np.real(beta),omega,'-')
plt.plot(np.imag(beta),omega,'--')
plt.plot(omega,omega,'-.')
plt.xlabel(r'$\dfrac{ c }{ _p }$')
plt.ylabel(r'$\dfrac{  }{ _p }$')
plt.xlim(1e-18,3.5)
plt.title("Dispersion Curve")
plt.legend([r"$\Re{(  )}$", r"$\Im{(  )}$", r"Light Line: $\omega = c\beta$"])
plt.grid()


# # Adding some Damping

# In[ ]:


with np.errstate(divide='ignore'):
    eq = sp.simplify(w *sp.sqrt((1.69+0.0j)*(9.84- 1/(w**2+1j*w*g))/(1.69+0.0j
    +(9.84-1/(w**2+1j*w*g)))))
    eq = eq.evalf(subs = {g:0.0074})
func = sp.lambdify(w,eq)
omega = np.linspace(0,2,1000)
beta = func(omega)
plt.figure(figsize = (12,8))
plt.plot(np.real(beta),omega,'-')
plt.plot(np.imag(beta),omega,'--')
plt.plot(omega,omega,'-.')
plt.xlabel(r'$\dfrac{ c }{ _p }$')
plt.ylabel(r'$\dfrac{  }{ _p }$')
plt.xlim(1e-18,1)
plt.ylim(1e-18,0.6)
plt.title("Dispersion Curve")
plt.legend([r"$\Re{(  )}$", r"$\Im{(  )}$", r"Light Line: $\omega = c\beta$"])
plt.grid()


# # $\mathcal{PT}$ Gain

# In[ ]:


def PTandGainSaturation():
```

```
#plt.close('all')

## Materials
eh = 1  # 9.84
wp = 1.367e16
g = 1.018e14
c = 3e8
kp = wp/c

## Setup frequency until wMetal
w = np.arange(0.3 * wp, 0.75 * wp, 0.001 * wp)

a = 1.69
ed = a
eS = 4

k0 = w / c
em = drudeModel(eh, wp, g, w)

## PT GAIN
gainPT = -1 / (2 * np.imag(em)) * (np.abs(em) ** 2 - np.sqrt(np.abs(em) ** 4 -
(2 * np.real(ed) * np.imag(em)) ** 2))
plt.figure(figsize = (12,8))
plt.plot(w / wp, -gainPT, '-')
plt.xlabel(r'$\omega/\omega_p$', fontsize = 16)
plt.ylabel(r'$\epsilon_{PT}$',fontsize = 16)
plt.grid(True)
plt.savefig("pt_gain_freq.png")



## DEFINE PT ACTIVE DIELECTRIC
ed = a + 1j * gainPT
edNoG = a
#print(-gainPT)

## Conditions
wspp = np.sqrt(wp ** 2 / (eh + np.real(a)) - g ** 2)
kz = k0 * np.sqrt(ed ** 2 / (em + ed))
kx = k0 * np.sqrt(ed * em / (ed + em))
kxNoG = k0 * np.sqrt(edNoG * em / (edNoG + em))
kd = k0 * np.sqrt(np.real(ed))
kS = k0 * np.sqrt(eS) * np.sin(0.905)

linn = np.linspace(0.2, 8, w.size)
plt.figure(figsize = (12,8))
plt.plot(np.real(kx) / kp, w / wp, 'b:', np.abs(np.imag(kx)) / kp, w / wp, 'r--'
, kd / kp, w / wp, 'y-.', linn, w / w * wspp / wp, 'g-')
plt.xlim(0,10)
setFigDisp()


L = 1 / (2 * np.abs(np.imag(kx))) * 1e6
LNoG = 1 / (2 * np.abs(np.imag(kxNoG))) * 1e6
#print(L)
linn = np.logspace(-4, 15, w.size)
plt.figure(figsize = (12,8))
plt.semilogy(w/wp,L, 'b-', w/wp,LNoG, 'g-', w / w * wspp / wp, linn, 'r--')
```

```
    setFigL()


def drudeModel(eh, wp, g, w):
    em = eh - wp ** 2 / (w ** 2 + 1j * w * g)
    return em

def setFigDisp():
    plt.legend([r'$\Re[\beta]$', r'$\Im[\beta]$', r'$k$-number in dielectric', r'$\
    omega_{sp}$'], loc='upper right')
    plt.title("Dispersion Curve")
    plt.xlabel(r'$\beta/k_p$', fontsize=16)
    plt.ylabel(r'$\omega/\omega_p$', fontsize=16)
    plt.axis('tight')
    plt.grid(True)
    plt.savefig("pt_disp_curve.png")
    plt.show()

def setFigL():
    plt.legend([r'$L$(theory)', r'$L$ with 0 gain(theory)', r'$\omega_{sp} = 0.61\
    omega_p$'], loc='upper right')
    plt.xlabel('$\omega/\omega_p$', fontsize=16)
    plt.ylabel('Propagation Length L ( m )', fontsize=16)
    plt.grid(True)
    plt.savefig("L_freq.png")
    plt.show()

PTandGainSaturation()


# # Multi-Layer Inteface

# # IMI Geometry

# In[2]:


wp = 2.2789e16 #silver = 1.3673 || aluminum = 2.2789   e16
gamma = 0.00 #normalized
a = 9e-9
c = 3e8
ed = 1
ed2 = 0.0
kp = wp/c
N = 1000

def funcspace(func,invfunc,start,end,step = 20):
    return func(np.linspace(invfunc(start),invfunc(end),step))

#wnorm = funcspace(lambda x: np.sqrt(x), lambda x: x**2, start = 0, end = 1, step =
    N)

wnorm = np.linspace(0,1,N)

dw = wnorm[1] - wnorm[0]

def f(bnorm,wnorm,gamma,ed2):
```

```
    return np.tanh(a*wp/c*np.sqrt((bnorm)**2 - ((1 - 1/(wnorm**2+1j*gamma*wnorm))*(
    wnorm)**2))) + np.sqrt(bnorm**2 -(ed+1j*ed2)*wnorm**2)*(1 - 1/(wnorm**2+1j*gamma
    *wnorm))/((ed+1j*ed2)*np.sqrt(bnorm**2 - (1 - 1/(wnorm**2+1j*gamma*wnorm))*(
    wnorm**2)))

def g(bnorm,wnorm,gamma,ed2):
    return 1/np.tanh(a*wp/c*np.sqrt((bnorm)**2 - ((1 - 1/(wnorm**2+1j*gamma*wnorm))
    *(wnorm)**2))) + np.sqrt(bnorm**2 -(ed+1j*ed2)*wnorm**2)*(1 - 1/(wnorm**2+1j*
    gamma*wnorm))/((ed+1j*ed2)*np.sqrt(bnorm**2 - (1 - 1/(wnorm**2+1j*gamma*wnorm))
    *(wnorm**2)))


# In[3]:


from tqdm.notebook import tqdm,trange

def temn(a, b, func, epsilon, args):

    count = 0
    f = 0
    funca = func(a,*args)
    funcb = func(b,*args)
    c = (b * funca - a * funcb) / (funca - funcb)
    #print(c)

    while abs(f := func(c,*args)) > epsilon:
        a = b
        b = c
        funca = func(a,*args)
        funcb = f
        c = (b * funca - a * funcb) / (funca - funcb)
        #print(c)
        count += 1

    #print(count)
    return c

odd_b = np.zeros(N, dtype= complex)
even_b = np.zeros(N, dtype = complex)

k = 0.001+0j
l = 0.0012+0j
for i in trange(1,N):

    sol = temn(k,l,f,1e-2,args = (wnorm[i],gamma,ed2))

    #while (np.abs(sol - odd_b[i-1]) > 100):
    #    k += 0.00001
    #    l += 0.00001
    #    sol = temn(k,l,f,1e-6,wnorm[i])


    odd_b[i] = sol
    k  = odd_b[i] + dw*(odd_b[i]-odd_b[i-1])/(wnorm[i] - wnorm[i-1]) + 0j
    l = k + 0.002

k = 0.01+0j
```

```
l = 0.012+0j
for i in trange(1,N):


    sol = temn(k,l,g,1e-6,args = (wnorm[i],gamma,ed2))
    #while ( np.abs(sol - even_b[i-1]) > 100):
    #    k += 0.00001
    #    l += 0.00001
    #    sol = temn(k,l,g,1e-6,wnorm[i])

    even_b[i] = sol
    k  = even_b[i] + dw*(even_b[i]-even_b[i-1])/(wnorm[i] - wnorm[i-1]) + 0j
    l = k + 0.02


#f(0.5149,0.5),g(0.5149,0.5)


# In[4]:


odd_index = (odd_b.real > 0) * (odd_b.real < 10)
even_index = (even_b.real > 0) * (even_b.real < 10)

odd_realb = odd_b.real[odd_index]
odd_realw = wnorm[odd_index]

even_realb = even_b.real[even_index]
even_realw = wnorm[even_index]

# vale a = 1.5
plt.plot(odd_realb,odd_realw,'--',color = 'green',label = 'odd mode')
plt.plot(even_realb,even_realw,'--',color = 'orange', label = 'even mode')
plt.plot(wnorm,wnorm,'--', color = 'black',label = 'Light line')
plt.xlabel(r'${ c }/{ _p }$')
plt.ylabel(r'$  / _p$ ')
#plt.xlim(0,6)
#plt.ylim(0,0.8)
plt.legend()
plt.grid()
#plt.savefig("multilayer_disp_relation_IMI.png")
plt.show()


# In[5]:


L = 1/(2*odd_b[odd_index].imag)


# # MIM Geometry

# In[2]:


loss = 0.01 #normalized
wp = 1.367e16
a = 1.5e-8
```

```
c = 3e8
ed = 1
kp = wp/c
N = 1000

def funcspace(func,invfunc,start,end,step = 20):
    return func(np.linspace(invfunc(start),invfunc(end),step))

#wnorm = funcspace(lambda x: np.sqrt(x), lambda x: x**2, start = 0, end = 1, step =
    N)

wnorm = np.linspace(0,1,N)

dw = wnorm[1] - wnorm[0]

def f(bnorm,wnorm):
    return np.tanh(a*wp/c*np.sqrt((bnorm)**2 - (ed*(wnorm)**2))) + np.sqrt(bnorm**2
    -(1 - 1/(wnorm**2+1j*loss*wnorm))*wnorm**2)*ed/((1 - 1/(wnorm**2+1j*loss*wnorm))
    *np.sqrt(bnorm**2 - ed*(wnorm**2)))

def g(bnorm,wnorm):
    return 1/np.tanh(a*wp/c*np.sqrt((bnorm)**2 - (ed*(wnorm)**2))) + np.sqrt(bnorm
    **2 -ed*wnorm**2)*(1 - 1/(wnorm**2+1j*loss*wnorm))/(ed*np.sqrt(bnorm**2 - (1-1/(
    wnorm**2+1j*loss*wnorm))*(wnorm**2)))
#f(0.81+0.8j,0.5),g(0.8098+0.1j,0.5)


# In[3]:


from tqdm.notebook import tqdm,trange

def temn(a, b, func, epsilon, omega):

    count = 0
    f = 0
    funca = func(a,omega)
    funcb = func(b,omega)
    c = (b * funca - a * funcb) / (funca - funcb)
    #print(c)

    while abs(f := func(c,omega)) > epsilon:
        a = b
        b = c
        funca = func(a,omega)
        funcb = f
        c = (b * funca - a * funcb) / (funca - funcb)
        #print(c)
        count += 1

    #print(count)
    return c

odd_b = np.zeros(N, dtype= complex)
even_b = np.zeros(N, dtype = complex)

k = 0.01+0j
l = 0.012+0j
```

```
for i in trange(1,N):

    sol = temn(k,l,f,1e-3,wnorm[i])

    #while (np.abs(sol - odd_b[i-1]) > 100):
    #    k += 0.00001
    #    l += 0.00001
    #    sol = temn(k,l,f,1e-6,wnorm[i])


    odd_b[i] = sol
    k  = odd_b[i] + dw*(odd_b[i]-odd_b[i-1])/(wnorm[i] - wnorm[i-1]) + 0j
    l = k + 0.02

k = 0.01+0j
l = 0.012+0j
for i in trange(1,N):


    sol = temn(k,l,g,1e-6,wnorm[i])
    #while ( np.abs(sol - even_b[i-1]) > 100):
    #    k += 0.00001
    #    l += 0.00001
    #    sol = temn(k,l,g,1e-6,wnorm[i])

    even_b[i] = sol
    k  = even_b[i] + dw*(even_b[i]-even_b[i-1])/(wnorm[i] - wnorm[i-1]) + 0j
    l = k + 0.5


#f(0.5149,0.5),g(0.5149,0.5)


# In[4]:


odd_index = (odd_b.real > 0) * (odd_b.real < 10)
even_index = (even_b.real > 0) * (even_b.real < 10)

odd_realb = odd_b.real[odd_index]
odd_realw = wnorm[odd_index]

even_realb = even_b.real[even_index]
even_realw = wnorm[even_index]

plt.plot(odd_realb,odd_realw,'--',color = 'green',label = 'odd mode')
plt.plot(even_realb,even_realw,'--',color = 'orange', label = 'even mode')
plt.plot(wnorm,wnorm,'--', color = 'black',label = 'Light line')
plt.xlabel(r'${ c }/{ _p }$')
plt.ylabel(r'$  / _p$ ')
#plt.xlim(0,3)
#plt.ylim(0,0.71)
plt.legend()
plt.grid()
#plt.savefig("multilayer_disp_relation_MIM.png")
plt.show()
```

---

[15]

Bibliography

[1] Hadiseh Alaeian and Jennifer A Dionne. Parity-time-symmetric plasmonic metamaterials. *Physical Review A*, 89(3):033829, 2014.

[2] C Athanasopoulos, M Mattheakis, and GP Tsironis. Enhanced surface plasmon polariton propagation induced by active dielectrics. *arXiv preprint arXiv:1311.5722*, 2013.

[3] E. N. Economou. Surface plasmons in thin films. *Phys. Rev.*, 182:539–554, Jun 1969.

[4] Jean-Jacques Greffet. Introduction to surface plasmon theory. In *Plasmonics: From Basics to Advanced Topics*, pages 105–148. Springer, 2012.

[5] Zhanghua Han and Sergey I Bozhevolnyi. Radiation guiding with surface plasmon polaritons. *Reports on Progress in Physics*, 76(1):016402, dec 2012.

[6] Ki Young Kim. *Plasmonics: Principles and Applications*. BoD–Books on Demand, 2012.

[7] Alex Krasnok, Nikita Nefedkin, and Andrea Alu. Parity-time symmetry and exceptional points: A tutorial. *arXiv preprint arXiv:2103.08135*, 2021.

[8] Stefan A Maier et al. *Plasmonics: fundamentals and applications*, volume 1. Springer, 2007.

[9] Marios Mattheakis, Efthimios Kaxiras, and GP Tsironis. Chapter graphene and active metamaterials: Theoretical methods and physical properties. 2017.

[10] Marios Mattheakis, Thomas Oikonomou, Mario I Molina, and George P Tsironis. Phase transition in $\mathcal{PT}$ symmetric active plasmonic systems. *IEEE Journal of Selected Topics in Quantum Electronics*, 22(5):76–81, 2015.

[11] JM Pitarke, VM Silkin, EV Chulkov, and PM Echenique. Theory of surface plasmons and surface-plasmon polaritons. *Reports on progress in physics*, 70(1):1, 2006.

[12] GC Psaltakis. Quantum many-particle systems. heraklion, 2012.

[13] Heinz Raether. Surface plasmons on gratings. *Surface plasmons on smooth and rough surfaces and on gratings*, pages 91–116, 2006.

[14] Dror Sarid and William A Challener. *Modern introduction to surface plasmons: theory, Mathematica modeling, and applications*. Cambridge University Press, 2010.

[15] Jasmin Smajic, Christian Hafner, Ludmila Raguin, Kakhaber Tavzarashvili, and Matthew Mishrikey. Comparison of numerical methods for the analysis of plasmonic structures. *Journal of Computational and Theoretical Nanoscience*, 6(3):763–774, 2009.

[16] Zongfu Yu, Georgios Veronis, Shanhui Fan, and Mark L Brongersma. Gain-induced switching in metal-dielectric-metal plasmonic waveguides. *Applied Physics Letters*, 92(4), 2008.